Published in final edited form as:

J Org Chem. 2020 February 07; 85(3): 1601–1613. doi:10.1021/acs.joc.9b02747.

Impact of Dehydroamino Acids on the Structure and Stability of Incipient 3_{10}-Helical Peptides

Daniel Joaquin, **Michael A. Lee**, **David W. Kastner**, **Jatinder Singh**, **Shardon T. Morrill**, **Gracie Damstedt**, **Steven L. Castle**

Department of Chemistry and Biochemistry, Brigham Young University, Provo, Utah 84602

Abstract

A comparative study of the impact of small, medium-sized, and bulky α,β-dehydroamino acids (ΔAAs) on the structure and stability of Balaram's incipient 3_{10}-helical peptide (**1**) is reported. Replacement of the *N*-terminal Aib residue of **1** with a ΔAA afforded peptides **2a–c** that maintained the 3_{10}-helical shape of **1**. In contrast, installation of a ΔAA in place of Aib-3 yielded peptides **3a–c** that preferred a β-sheet-like conformation. The impact of the ΔAA on peptide structure was independent of size, with small (ΔAla), medium-sized (*Z*-ΔAbu), and bulky (ΔVal) ΔAAs exerting similar effects. The proteolytic stabilities of **1** and its analogs were determined by incubation with Pronase. Z-ΔAbu and ΔVal increased the resistance of peptides to proteolysis when incorporated at the 3-position and had negligible impact on stability when placed at the 1-position, whereas ΔAla-containing peptides degraded rapidly regardless of position. Exposure of peptides **2a–c** and **3a–c** to the reactive thiol cysteamine revealed that ΔAla-containing peptides underwent conjugate addition at room temperature, while *Z*-ΔAbu- and ΔVal-containing peptides were inert even at elevated temperatures. These results suggest that both bulky and more accessible medium-sized ΔAAs should be valuable tools for bestowing rigidity and proteolytic stability on bioactive peptides.

Graphical Abstract

scastle@chem.byu.edu.

Supporting Information Available.

Data from proteolysis assays and peptide HPLC traces, tabulated 1D and 2D NMR data of peptides **1**, **2a–c**, and **3a–c**, tabulated restraints and parameters used in structural calculations, structures of peptides **1**, **2a–c**, and **3a–c** calculated using NMR data, ROESY spectrum snapshots, and copies of ^{1}H and ^{13}C NMR spectra for all new compounds. This material is available free of charge via the Internet at http://pubs.acs.org.

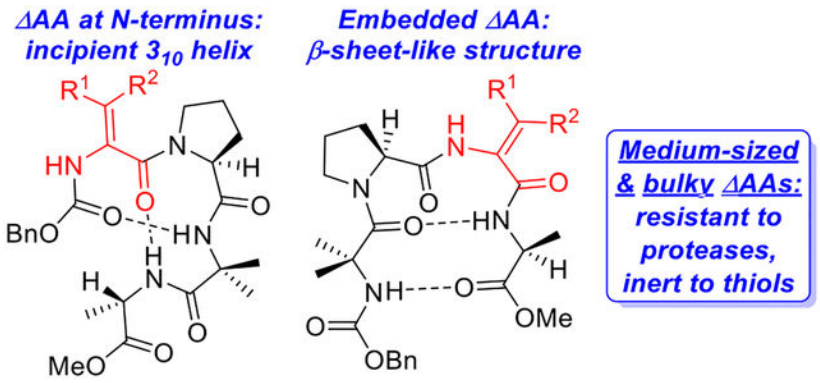

INTRODUCTION

The great potential of peptides as therapeutic agents[1] continues to inspire the discovery of new methods for increasing their short half-lives, which are caused by facile proteolytic degradation and rapid renal clearance. A host of structural motifs including peptoids,[2] β and α/β peptides,[3] stapled peptides,[4] hydrogen bond surrogates,[5] γAA-peptides,[6] D-peptides,[7] α,α-disubstituted amino acids,[8] *N*-amino peptides,[9] and β-turn mimics[10] can decrease their susceptibility to proteolysis. Additionally, techniques such as PEGylation,[11] conjugation to albumin or antibody fragments,[12] and anchoring to plasma membranes[13] are effective at slowing renal clearance and/or proteolysis. In spite of these successes, only a modest number of peptide drugs is currently reaching the market.[14] Thus, more strategies for increasing the half-lives of these potential therapeutics are urgently required.

In seminal work conducted 35–40 years ago, Stammer and co-workers established that α,β-dehydroamino acids (ΔAAs) such as ΔAla, *Z*-ΔPhe, and *Z*-ΔLeu could improve the proteolytic stability of the enkephalin peptide hormones.[15] In regards to ΔPhe and ΔLeu, this phenomenon can be attributed to the $A_{1,3}$ strain caused by the alkene, which limits the conformational freedom of these residues and increases the rigidity of peptides that contain them. This rigidity favors folded states instead of random coil conformations and leads to greater stability since folded peptides undergo proteolysis more slowly than unfolded peptides.[16] Subsequent to Stammer's pioneering investigations, Chauhan[17,18] and others[19] studied the impact of ΔAAs containing trisubstituted alkenes (e.g., ΔPhe, ΔLeu) on peptide structure. In general, these residues promote the formation of β-turns or 3_{10} helices (Figure 1). In fact, Dong and co-workers recently exploited the turn-inducing properties of ΔPhe as an aid to cyclizing pentapeptides.[20] This ΔAA and its analogs have been inserted into the backbones of bioactive peptides with promising results.[21] ΔPhe and other ΔAAs that incorporate trisubstituted alkenes are typically encountered as the more stable *Z*-isomers due to challenges in constructing the *E*-isomers[22] and *E*-to-*Z* isomerization that often occurs during peptide coupling reactions.[23]

Despite their presence in bioactive peptides including the yaku'amides,[24] phomopsins,[25] and myxovalargin A,[26] bulky dehydroamino acids such as ΔVal and ΔIle that contain tetrasubstituted alkenes have been less studied than their counterparts with trisubstituted *Z*-alkenes (Figure 1).[27,28] We hypothesized that the elevated $A_{1,3}$ strain characteristic of bulky

ΔAAs would render them more effective than smaller ΔAAs at rigidifying peptides and increasing their proteolytic stability. However, this strain also makes them more difficult to incorporate into peptides than their smaller relatives. A few years ago, we developed a protocol for synthesizing peptides containing ΔVal and its bis-homolog dehydroethylnorvaline (ΔEnv) via solid-phase peptide synthesis.[29] We applied this method to the construction of β-hairpins and demonstrated that inserting bulky ΔAAs into these peptides leads to an increased preference for the folded state as well as substantially higher proteolytic stability.[30] The synthetic challenges that we faced during this endeavor, which included construction of congested azlactone dipeptides and sluggish couplings of these species, caused us to wonder how the effect of bulky ΔAAs on peptide structure and stability compared to that of medium-sized ΔAAs with trisubstituted alkenes. Specifically, we were unsure if the extra effort required to furnish peptides containing bulky ΔAAs was worthwhile. Comparisons of these two types of ΔAAs in the literature have been limited to studies of individual amino acids[27f–h] or dipeptides[27a] that are too small to exhibit secondary structure. Accordingly, we resolved to examine the impact of small (i.e., ΔAla), medium-sized (i.e., dehydro-2-aminobutyric acid or ΔAbu), and bulky ΔAAs (i.e., ΔVal) on the structure and stability of incipient 3_{10}-helical peptides.[31] Herein, we report the results of this investigation.

RESULTS AND DISCUSSION

In 1979, Balaram and co-workers synthesized tetrapeptide **1** (Figure 2) and studied its structure using X-ray crystallography and NMR spectroscopy. They determined that **1** forms two overlapping β-turns in solution and in the solid state, representing an incipient 3_{10} helix due to the presence of consecutive ($i \rightarrow i + 3$) hydrogen bonds.[31] This compound is well-suited as a system for studying the impacts of different ΔAAs on peptide structure and stability, as the turn-inducing properties of these residues should cause subtle yet measurable perturbations to its secondary structure. Moreover, the short and simple sequence of **1** should render its ΔAA-containing variants synthetically accessible and relatively straightforward to study via NMR spectroscopy. Thus, we targeted peptides **2** (Figure 2) in which the Aib-1 residue is replaced by ΔVal (**2a**), ΔAla (**2b**), or Z-ΔAbu (**2c**) in order to probe the impact of these ΔAAs when they are inserted at the ($i + 1$) position of one of the β-turns contained in the incipient 3_{10} helix. Similarly, peptides **3** would permit evaluation of the effect of ΔAAs when placed at the ($i + 2$) position.

The synthesis of analog **2a** incorporating a bulky ΔAA in place of the Aib-1 residue in **1** commenced with the construction of tripeptide **5** via coupling of Aib-Ala-OMe (**4**) and Cbz-Pro (Scheme 1). The moderate yield is presumably due to the steric hindrance of the two coupling partners. ΔVal derivative **7** was generated in good yield by using Martin sulfurane to dehydrate β-OHVal derivative **6**, which is readily available via OsO_4-catalyzed aminohydroxylation.[29,32] Saponification of **7** was sluggish owing to the $A_{1,3}$ strain caused by the β-methyl groups, with two days required to obtain complete conversion to acid **8**. Coupling of this acid with the amine derived from hydrogenolysis of tripeptide **5** furnished the targeted tetrapeptide **2a** in reasonable yield considering bulkiness of the reactants.

Preparation of ΔAla-containing analog **2b** proceeded smoothly as outlined in Scheme 2. Dehydration of the dipeptide Cbz-Ser-Pro-OMe (**9**) was accomplished by mesylation of the primary alcohol followed by exposure to DBU and heat.[33] No racemization of the Pro residue was detected under these conditions. Saponification of the resulting ΔAla-containing dipeptide and coupling with dipeptide **4** delivered **2b** in an acceptable yield considering the hindered nature of the reactants.

The synthesis of variant **2c** possessing the medium-sized trisubstituted ΔAA *Z*-ΔAbu required coupling of dipeptides **4** and **11**, which was a challenging reaction (Scheme 3). Brief attempts at optimization revealed that HBTU could promote the coupling in low but consistent yields. While it is possible that either protecting the secondary alcohol of **11** or inverting the order of the dehydration and coupling steps could have resulted in better yields, we elected not to explore these alternatives since we were able to generate the required amounts of **2c** using the short sequence shown in Scheme 3. This peptide was produced in modest yield by dehydrating tetrapeptide **12** with the Martin sulfurane.[22a]

Analog **3a**, which contains ΔVal instead of the Aib-3 residue of Balaram's peptide, was synthesized as shown in Scheme 4. The dipeptide Cbz-Aib-Pro was coupled with racemic β-OH-Val derivative **14** to afford tripeptide **15** in good yield. Saponification of this peptide was followed by dehydration and azlactone formation utilizing NaOAc and Ac_2O in THF.[30] Ring-opening and coupling of the hindered azlactone intermediate was difficult. A brief survey of conditions revealed that serviceable yields of tetrapeptide **3a** could be obtained by first hydrolyzing the azlactone through treatment with NaOH and then employing PyBOP to mediate coupling with Ala-OMe.[34]

Construction of variant **3b** wherein the Aib-3 residue of **1** is replaced by ΔAla is summarized in Scheme 5. Hydrogenolysis of the dipeptide Cbz-Ser-Ala-OMe (**16**) was followed by coupling with dipeptide **13**, furnishing tetrapeptide **17** in moderate yield. As in the coupling of **11**, protection of the alcohol moiety in **16** was eschewed in favor of a short and direct synthetic route to **3b**. Mesylation and elimination of the primary alcohol in **17** was lower-yielding than the analogous transformation of dipeptide **9** (see Scheme 2), as **3b** was obtained in 36% yield.

Preparation of analog **3c** possessing *Z*-ΔAbu in place of Aib-3 commenced with coupling of **13** to dipeptide **18** (Scheme 6). We suspect that steric hindrance is the primary reason for the low yields of this reaction. Exposure of the resulting tetrapeptide **19** to the Martin sulfurane afforded **3c**. The poor yields that we encountered while synthesizing some of the analogs of **1** are indicative of limits in current methods for constructing hindered peptides containing ΔAAs. While our concise routes enabled us to overcome these problems and generate sufficient quantities of the small target peptides **2** and **3**, we plan to address these limitations in future studies.

The ^1H NMR spectra of **2a–c** and **3a–c** in $CDCl_3$ solutions provided evidence of a rigid and well-defined major conformation for each peptide. The peptides in each series exhibit similar spectral characteristics, suggesting that the position of the ΔAA in the chain has a larger impact on peptide structure than the nature of the ΔAA (i.e., small, medium-sized, or

bulky). Monitoring of the NH moieties of **2a–c** in $CDCl_3$ solutions doped with D_2O revealed rapid H–D exchange of the ΔAA carbamate NH and negligible H–D exchange of the Aib and Ala amide NH groups. These observations are consistent with the 3_{10}-helical pattern of intramolecular hydrogen bonds shown in Figure 3. In contrast, analogous experiments conducted with **3a–c** showed rapid H–D exchange of the ΔAA amide NH and minimal H–D exchange of the Aib carbamate NH and the Ala amide NH groups. These data fit the β-sheet-like pattern of intramolecular hydrogen bonds depicted in Figure 3. Interestingly, in $CDCl_3$ solutions the ΔAA residues do not participate in intramolecular hydrogen bonding regardless of their position in the chain.

In an attempt to determine the impact of a polar environment on the hydrogen bonding patterns of **2** and **3**, we conducted variable-temperature ^1H NMR experiments with solutions of these peptides in DMSO-d_6. In this solvent, only the Ala amide NH groups of **2a–c**, **3a**, and **3c** participate in intramolecular hydrogen bonding. Apparently, the intramolecular hydrogen bonds involving the Aib amide or carbamate NH groups that are present in the less polar $CDCl_3$ solvent are weak enough to be disrupted by interactions with the highly polar DMSO-d_6 solvent molecules. Surprisingly, only the ΔAla amide NH of peptide **3b** forms an intramolecular hydrogen bond in DMSO-d_6 solution. Perhaps the absence of $A_{1,3}$ strain in the small ΔAla residue allows this peptide to adopt a conformation in a strongly polar solvent that is unavailable to the other peptides with larger ΔAA residues and intrinsic $A_{1,3}$ strain.

NOE-restrained structural calculations using the program CYANA 2.1[35] provided insights into the solution structures of **1** and its analogs. First, ROESY spectra were acquired for each compound with a mixing time of 200 ms. The resulting cross-peaks were then converted to upper-distance constraints. A standard simulated annealing calculation was then performed for 100 conformers of each peptide with the upper-limit file and experimentally determined hydrogen bonding pattern as input. The ten structures with the lowest objective target function were then superimposed to create a final ensemble for each peptide, which was then analyzed based on structure and RMSD values using the molecular visualization software VMD. These ensembles are shown in Figure 4. The parent peptide **1** exhibits the highest RMSD value of 1.154 Å, suggesting that it has more conformational freedom than its analogs. As anticipated from the intramolecular hydrogen bonding data, the peptides with a ΔAA in place of Aib-1 (i.e., **2a–c**) form incipient 3_{10}-helical structures and the peptides with a ΔAA in place of Aib-3 (i.e., **3a–c**) resemble β-turns. These structural data demonstrate that the position of the ΔAA plays an important role in determining the conformation preferred by each analog.

Peptides **3a–c** exhibit lower RMSD values than peptides **2a–c**, indicating that placement of a ΔAA at the Aib-3 position leads to a greater increase in rigidity than does placement at the Aib-1 position. Interestingly, the conformations of the ΔVal and *Z*-ΔAbu residues in peptides of the same series are quite similar (i.e., **2a** and **2c**, **3a** and **3c**). However, the *Z*-ΔAbu-containing analogs **2c** and **3c** exhibit higher RMSD values than the corresponding ΔVal-containing analogs **2a** and **3a**. While both residues apparently prefer similar low-energy conformations, it appears that the additional $A_{1,3}$ strain inherent in a tetrasubstituted alkene relative to a trisubstituted alkene destabilizes the high-energy conformations of ΔVal to a

greater degree than those of *Z*-ΔAbu. Thus, our data suggest that medium-sized and bulky ΔAAs exert similar effects on the structures of peptides, but that bulky ΔAAs impart more rigidity.

The stability of **1** and its analogs to proteolytic degradation was determined by treating the peptides with Pronase, a cocktail of proteases from *Streptomyces griseus* that aggressively cleaves peptide bonds in a nonspecific fashion.[36] Since **1** is relatively stable to proteolysis due to its two Aib residues, a high concentration of Pronase was required for it to degrade on a reasonable timescale. As a result, the kinetics of peptide degradation were affected by self-proteolysis of the enzymes. Although this prevented us from measuring half-lives, we were able to compare the amount of each peptide that remained after 30 minutes of incubation with Pronase as recorded in Table 1. Peptides **2b** and **3b** containing ΔAla were significantly more labile than Balaram's peptide, as the relative abundance of the former peptides after 30 minutes of exposure to Pronase was ca. 10–30% that of the latter. Thus, it is clear that Aib is more effective than ΔAla at protecting peptides from proteolysis. Interestingly, the effects of *Z*-ΔAbu and ΔVal were dependent on their location in the peptide chain. Analogs **2a** and **2c** possessing a ΔAA at the *N*-terminus were equally or slightly less stable than **1**, respectively. In contrast, variants **3a** and **3c** in which the ΔAA replaces Aib-3 were more stable than **1**, as approximately twice as much of each remained after exposure to Pronase for 30 minutes. While the ΔVal-containing peptides **2a** and **3a** were slightly more stable than the *Z*-ΔAbu-containing peptides **2b** and **3b**, the differences in performance were not dramatic. Although a more detailed and comprehensive study would be required to generate firm conclusions, these data suggest that *Z*-ΔAbu and ΔVal might confer comparable increases in proteolytic stability upon peptides that contain them. Importantly, our results show that in some cases the stabilizing impact of these two ΔAAs can exceed that of the α,α-disubstituted residue Aib.

Conventional wisdom indicates that ΔAAs are reactive electrophiles that undergo conjugate additions by biological nucleophiles such as thiols.[37] In fact, enzyme-catalyzed conjugate additions of thiols to ΔAla and ΔAbu are involved in the biosynthesis of lantibiotics.[38] However, a close look at the literature reveals that uncatalyzed conjugate additions of thiols to ΔAAs larger than ΔAla typically require large excesses of thiol to proceed.[39] Alternatively, placement of the ΔAA at the *C*-terminus of a peptide instead of embedded within the backbone can increase its electrophilicity.[40] Based on these prior results, we postulated that steric hindrance at the β-carbon atom would significantly attenuate the reactivity of medium-sized and bulky ΔAAs to thiols in the absence of enzymes. We probed this hypothesis by exposing solutions of **2a–c** and **3a–c** in DMSO-d_6 to ca. 2 equiv of cysteamine, a highly nucleophilic thiol.[41] As anticipated, ΔAla-containing peptides **2b** and **3b** were steadily consumed under these conditions. The decomposition of cysteamine in solution complicated our efforts to calculate half-lives for these reactions. Nonetheless, it was clear that **3b** was consumed more rapidly than **2b**, as 65% of the former and 93% of the latter remained after 40 minutes of incubation at room temperature.

In contrast, ΔVal-containing peptides **2a** and **3a** as well as *Z*-ΔAbu-containing peptides **2c** and **3c** were inert to cysteamine at temperatures up to 100 °C, at which point the thiol decomposed completely. Thus, neither of these residues is reactive to thiols when embedded

within a peptide (i.e., not located at the *C*-terminus). While further investigation is warranted, these results suggest that both medium-sized and bulky ΔAAs can be incorporated into bioactive peptides without fear of *in vivo* degradation due to conjugate addition. Interestingly, subjection of α-methylene-γ-butyrolactone to cysteamine caused complete consumption of the electrophile within 5 minutes at room temperature. This result shows that ΔAla-containing peptides **2b** and **3b** are only modestly reactive to cysteamine by comparison, implying that peptides including this residue might also be useful for some biological applications.

CONCLUSIONS

In an effort to compare the impacts of small (i.e., ΔAla), medium-sized (i.e., *Z*-ΔAbu), and bulky ΔAAs (i.e., ΔVal) on peptide structure and stability, we synthesized ΔAA-containing analogs **2a–c** and **3a–c** of Balaram's incipient 3_{10}-helical peptide **1**. The different types of ΔAAs exerted similar effects on conformation in $CDCl_3$ solution according to NOE-restrained structural calculations. Variants **2a–c** possessing a ΔAA in place of Aib-1 all preferred the 3_{10}-helical shape of the original peptide, whereas analogs **3a–c** with a ΔAA replacing Aib-3 all adopted a β-sheet-like orientation instead. Thus, the location of the ΔAA in the backbone played a larger role than the size of the residue in determining the structures of the peptides. The proteolytic stabilities of **1** and its analogs were evaluated by exposure to Pronase. ΔAla-containing analogs **2b** and **3b** were degraded rapidly, demonstrating that this small ΔAA does not protect peptides from proteolysis. *Z*-ΔAbu and ΔVal increased proteolytic stability to similar degrees, with the most pronounced effect (ca. twice as stable as **1**) occurring when the ΔAA replaced Aib-3. Intriguingly, peptides containing *Z*-ΔAbu and ΔVal were completely unreactive to conjugate addition by the potent nucleophile cysteamine at temperatures up to 100 °C, whereas ΔAla-containing peptides reacted at room temperature. The comparable impacts of *Z*-ΔAbu and ΔVal on proteolytic stability suggests that the former residue is likely to be preferred to the latter due to its relative ease of synthesis, except in cases where the increased rigidity caused by the elevated $A_{1,3}$-strain in ΔVal is desired. The inertness of both of these residues to thiols suggests that they can be incorporated into bioactive peptides without fear of degradation by biological nucleophiles. While we hope that these conclusions will be valid with peptides larger than **2** and **3**, further experimentation is required to confirm this premise. When viewed as a whole, our results provide indications of the promise of medium-sized and bulky ΔAAs as tools for imparting rigidity and proteolytic stability to peptides. Future studies will focus on the impact of ΔAAs on other secondary structures as well as the synthesis and study of additional ΔAAs including medium-sized ΔAAs that are larger than ΔAbu (e.g., ΔPhe and ΔLeu).[42]

EXPERIMENTAL SECTION

General Details.

Dimethylformamide and tetrahydrofuran were dried by passage through cylinders of activated alumina. Chloroform was dried over 4 Å molecular sieves and Na_2SO_4 under Ar overnight. An oil bath was used to heat reactions that required elevated temperatures to proceed. Flash chromatography was conducted using 60–230 mesh silica gel. ^{1}H NMR

spectra were acquired on a 500 MHz spectrometer with chloroform (7.27 ppm) as internal reference. Signals are reported as follows: s (singlet), d (doublet), t (triplet), q (quartet), quint (quintet), dd (doublet of doublets), br s (broad singlet), m (multiplet). ^{13}C NMR spectra were acquired on a spectrometer operating at 125 MHz with chloroform (77.23 ppm) as internal reference. Infrared spectra were obtained on an FT-IR spectrometer. MS data were obtained using ESI techniques.

Methyl (2-amino-2-methylpropanoyl)-l-alaninate (4).

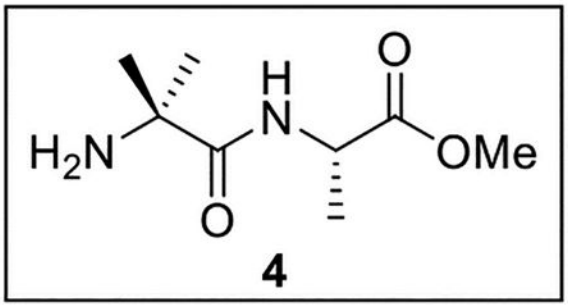

4

A solution of Z-Aib-OH (1.5034 g, 6.34 mmol) in anhydrous THF–DMF (5:1, 48 mL) at 0 °C under Ar was treated sequentially with Ala-OMe (944.5 mg, 6.77 mmol, 1.1 equiv), HOBt (ca. 20% H_2O content, 1.2988 g, 7.69 mmol, 1.2 equiv), EDC·HCl (1.7356 g, 9.05 mmol, 1.4 equiv), and $NaHCO_3$ (1.2811 g, 15.25 mmol, 2.4 equiv). The resulting mixture was slowly warmed to rt and stirred for 24 h. The reaction was quenched by the addition of sat aq $NaHCO_3$ (25 mL), diluted with H_2O (30 mL), and extracted with EtOAc (5 × 40 mL). The combined organic layers were dried (Na_2SO_4) and concentrated *in vacuo*. Flash chromatography (200 mL of SiO_2, 0–30% EtOAc in hexanes gradient elution) afforded Z-Aib-Ala-OMe (1.936 g, 6.01 mmol, 95%) as a white solid: $[\alpha]^{25}_D$ −3.3 (*c* 1.2, $CHCl_3$); ^1H NMR ($CDCl_3$, 500 MHz) δ 7.38–7.31 (m, 5H), 6.80 (br s, 1H), 5.29 (br s, 1H), 5.11 (s, 2H), 4.59–4.52 (m, 1H), 3.75 (s, 3H), 1.56 (s, 3H), 1.54 (s, 3H), 1.38 (br s, 3H); $^{13}C\{^1H\}$ NMR ($CDCl_3$, 125 MHz) δ 173.8, 173.4, 155.0, 136.2, 128.6 (2C), 128.2, 128.1 (2C), 66.8, 56.9, 52.4, 48.2, 25.7, 25.2, 18.2; IR (film) υ_{max} 3327, 2998, 1725, 1660, 1522, 1454, 1255, 1074 cm^{-1}; HRMS (ESI-TOF) *m*/*z*: $[M + H]^+$ Calcd for $C_{16}H_{22}N_2O_5H$ 323.1607; Found 323.1600.

A solution of Z-Aib-Ala-OMe (1.001 g, 3.11 mmol) in CH_3OH (10.0 mL) was treated with 10% Pd/C (501.1 mg, 0.5 wt equiv) at rt under Ar. The resulting mixture was stirred at rt under H_2 (500 psi) for 72 h, then diluted with H_2O (10 mL) and extracted with EtOAc (4 × 6 mL). The combined organic layers were dried (Na_2SO_4) and concentrated *in vacuo*. The crude Aib-Ala-OMe (**4**, 559.6 mg, 2.97 mmol, 96%) was used directly in subsequent coupling reactions without further purification.

Benzyl (*S*)-2-((1-(((*S*)-1-methoxy-1-oxopropan-2-yl)amino)-2-methyl-1-oxopropan-2-yl)carbamoyl)pyrrolidine-1-carboxylate (5).

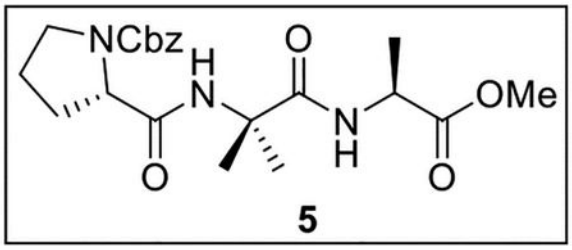

A solution of Z-Pro-OH (44.8 mg, 0.180 mmol) in anhydrous THF–DMF (5:1, 6 mL) at 0 °C under Ar was treated sequentially with **4** (35.4 mg, 0.188 mmol, 1.0 equiv), HOBt (ca. 20% H_2O content, 38.3 mg, 0.227 mmol, 1.3 equiv), EDC·HCl (50.5 mg, 0.263 mmol, 1.5 equiv), and $NaHCO_3$ (38.3 mg, 0.456 mmol, 2.5 equiv). The resulting mixture was slowly warmed to rt and stirred for 24 h. The reaction was quenched by the addition of sat aq $NaHCO_3$ (3 mL), diluted with H_2O (6 mL), and extracted with EtOAc (5 × 10 mL). The combined organic layers were dried (Na_2SO_4) and concentrated *in vacuo*. Flash chromatography (100 mL of SiO_2, 0–80% EtOAc in hexanes gradient elution) afforded **5** (39.3 mg, 0.0937 mmol, 52%) as a white film: $[\alpha]^{25}_D$ −55 (*c* 0.78, $CHCl_3$); ^{1}H NMR ($CDCl_3$, 500 MHz) δ 7.38–7.30 (m, 5H), 7.22 (br s, 1H), 6.67 (br s, 1H), 5.18 (d, *J* = 12.2 Hz, 1H), 5.12 (d, *J* = 12.4 Hz, 1H), 4.52 (quint, *J* = 7.2 Hz, 1H), 4.20–4.15 (m, 1H), 3.73 (s, 3H), 3.60–3.54 (m, 1H), 3.52–3.45 (m, 1H), 2.25–2.14 (m, 1H), 2.08–2.00 (m, 1H), 1.95–1.87 (m, 2H), 1.55 (s, 3H), 1.49 (s, 3H), 1.37 (d, *J* = 7.2 Hz, 3H); ^{13}C{^{1}H} NMR ($CDCl_3$, 125 MHz) δ 173.6, 173.5, 171.4, 156.0, 136.3, 128.6 (2C), 128.2, 127.8 (2C), 67.4, 61.2, 57.3, 52.2, 48.3, 47.1, 28.9, 26.5, 24.7, 24.4, 17.8; IR (film) υ_{max} 3319, 2997, 1751, 1685, 1519, 1421, 1357, 1174, 1110 cm^{-1}; HRMS (ESI-TOF) *m*/*z*: [M + H]$^+$ Calcd for $C_{21}H_{29}N_3O_6H$ 420.2135; Found 420.2127.

Ethyl 2-(((Benzyloxy)carbonyl)amino)-3-methylbut-2-enoate (7).

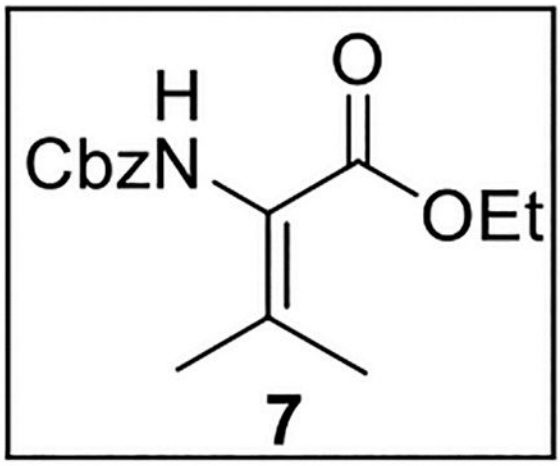

A solution of **6**[32] (172 mg, 0.582 mmol) in anhydrous $CHCl_3$ (3 mL) at 0 °C was treated with Martin sulfurane (783.2 mg, 1.16 mmol, 2.0 equiv) and stirred at 0 °C to rt for 1 h. The

mixture was then dried (Na_2SO_4) and concentrated *in vacuo*. Flash chromatography (150 mL of SiO_2, 0–1.5% MeOH in CH_2Cl_2 gradient elution) afforded **7** (139.4 mg, 0.503 mmol, 86%) as a yellow oil: ^{1}H NMR ($CDCl_3$, 500 MHz) δ 7.41–7.30 (m, 5H), 5.99 (br s, 1H), 5.16 (s, 2H), 4.26–4.19 (m, 2H), 2.19 (s, 3H), 1.91 (s, 3H), 1.31–1.25 (m, 3H); ^{13}C{^{1}H} NMR ($CDCl_3$, 125 MHz) δ 164.9, 159.9, 145.6, 136.3, 128.5 (2C), 128.2, 128.1 (2C), 126.2, 67.1, 60.8, 22.5, 21.3, 14.2; IR (film) υ_{max} 3324, 2924, 1715, 1499, 1454, 1373, 1308, 1249, 1090 cm^{-1}; HRMS (ESI-TOF) *m*/*z*: [M + H]$^+$ Calcd for $C_{15}H_{19}NO_4H$ 278.1392; Found 278.1383.

2-(((Benzyloxy)carbonyl)amino)-3-methylbut-2-enoic acid (8).

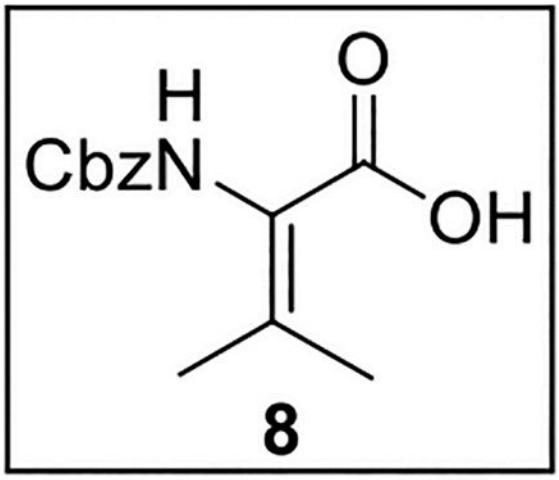

A solution of **7** (22.0 mg, 0.0793 mmol) in THF–EtOH–H_2O (3:2:1, 3 mL) at rt was treated with LiOH·H_2O (15.2 mg, 0.362 mmol, 4.6 equiv). The resulting mixture was stirred at 50 °C for 48 h. The reaction was acidified using 1N HCl until pH ~2, and the mixture was then extracted with EtOAc (4 × 10 mL). The combined organic layers were washed with brine (8 mL), dried (Na_2SO_4), and concentrated *in vacuo*. The crude acid **8** (20 mg, 0.079 mmol, quant.), was obtained as a yellow oil and used in subsequent reactions without further purification.

Methyl (2-((*S*)-1-(2-(((Benzyloxy)carbonyl)amino)-3-methylbut-2-enoyl)pyrrolidine-2-carboxamido)-2-methylpropanoyl)-l-alaninate (2a).

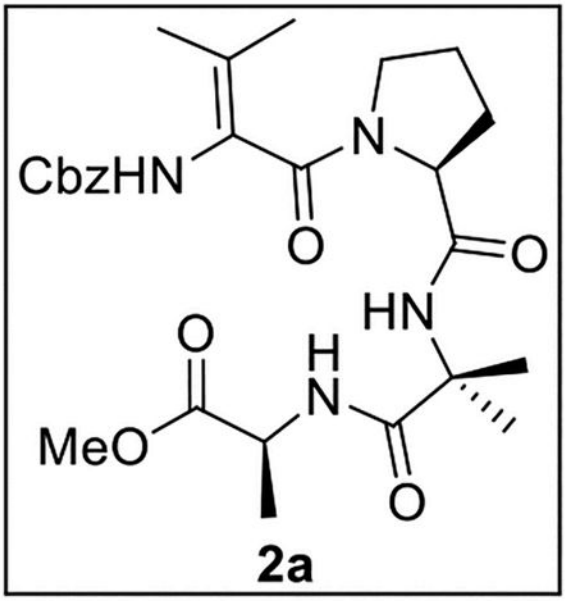

A solution of **5** (34.3 g, 0.0818 mmol) in MeOH (4 mL) at rt under Ar was treated with 10% Pd/C (21.5 mg, 0.63 wt equiv). The resulting mixture was stirred at rt under H_2 (500 psi) for 72 h, then filtered through Celite, dried (Na_2SO_4), and concentrated *in vacuo*. The crude Pro-Aib-Ala-OMe product (18.5 mg, 0.0648 mmol, 79%) was used directly in subsequent coupling reactions without further purification.

A solution of acid **8** (20.0 mg, 0.0802 mmol, 1.2 equiv) in anhydrous THF–DMF (6:1, 3.5 mL) at 0 °C under Ar was treated sequentially with Pro-Aib-Ala-OMe (18.5 mg, 0.0648 mmol, 1.0 equiv), HOBt (ca. 20% H_2O content, 17.0 mg, 0.101 mmol, 1.6 equiv), EDC·HCl (21.7 mg, 0.113 mmol, 1.7 equiv), and $NaHCO_3$ (14.6 mg, 0.174 mmol, 2.7 equiv). The resulting mixture was stirred at 0 °C to rt for 48 h. The reaction was quenched by the addition of sat aq $NaHCO_3$ (3 mL) and diluted with H_2O (6 mL), and the mixture was then extracted with EtOAc (5 × 10 mL). The combined organic layers were dried (Na_2SO_4) and concentrated *in vacuo*. Flash chromatography (100 mL of SiO_2, 0–80% EtOAc in hexanes gradient elution) afforded **2a** (15.8 mg, 0.0306 mmol, 47%) as a white solid: $[\alpha]^{25}_D$ −16 (*c* 0.9, $CHCl_3$); ^{1}H NMR ($CDCl_3$, 500 MHz) δ 7.41 (br s, 1H), 7.40–7.34 (m, 5H), 7.33 (br s, 1H), 6.35 (s, 1H), 5.14 (d, *J* = 12.2 Hz, 1H), 5.06 (d, *J* = 12.2 Hz, 1H), 4.53–4.48 (m, 2H), 3.69 (s, 3H), 3.66–3.61 (m, 1H), 3.55–3.49 (m, 1H), 2.35–2.28 (m, 1H), 2.18–2.09 (m, 1H), 2.04–1.91 (m, 2H), 1.76 (s, 3H), 1.73 (s, 3H), 1.55 (s, 3H), 1.51 (s, 3H), 1.37 (d, *J* = 7.2 Hz, 3H); ^{13}C{^{1}H} NMR ($CDCl_3$, 125 MHz) δ 174.4, 173.4, 170.6, 166.7, 153.9, 135.4, 128.7 (2C), 128.6, 128.1 (2C), 124.6, 122.7, 67.6, 61.0, 57.3, 52.1, 48.4, 48.3, 29.0, 25.6, 25.4, 24.5, 19.8, 18.3, 17.6; IR (film) υ_{max} 3322, 2924, 1640, 1518, 1445, 1240, 1261 cm^{-1}; HRMS (ESI-TOF) *m*/*z*: [M + H]$^+$ Calcd for $C_{26}H_{36}N_4O_7H$ 517.2662; Found 517.2677.

Methyl ((Benzyloxy)carbonyl)-l-serylprolinate (9).

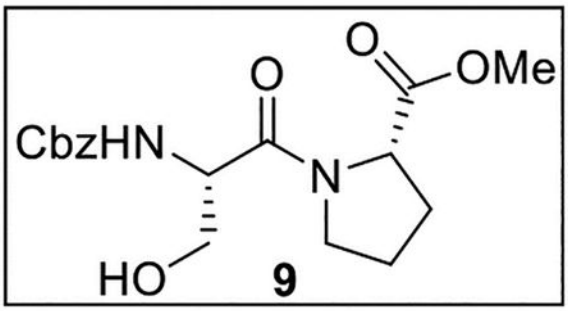

A solution of Z-Ser-OH (500.5 mg, 2.09 mmol) in anhydrous THF–DMF (5:1, 18 mL) under Ar at 0 °C was treated sequentially with Pro-OMe·HCl (363.4 mg, 2.19 mmol, 1.05 equiv), HOBt (ca. 20% H_2O content, 458.8 mg, 2.72 mmol, 1.3 equiv), EDC·HCl (680.9 mg, 3.55 mmol, 1.7 equiv), and $NaHCO_3$ (403.7 mg, 4.81 mmol, 2.3 equiv). The resulting mixture was slowly warmed to rt and stirred for 24 h. The reaction was quenched by the addition of sat aq $NaHCO_3$ (15 mL), diluted with H_2O (25 mL), and extracted with EtOAc (4 × 25 mL). The combined organic layers were dried (Na_2SO_4) and concentrated *in vacuo*. Flash chromatography (185 mL of SiO_2, 0–5% MeOH in CH_2Cl_2 gradient elution) afforded **9** (597.3 mg, 1.70 mmol, 81%) as a white solid: $[\alpha]^{25}_D$ −25 (*c* 0.6, $CHCl_3$); ^{1}H NMR ($CDCl_3$, 500 MHz) δ 7.36–7.29 (m, 5H), 5.95–5.89 (m, 1H), 5.09 (s, 2H), 5.07 (br s, 1H), 4.70–4.64 (m, 1H), 4.59–4.55 (m, 1H), 3.92–3.88 (m, 1H), 3.86–3.79 (m, 1H), 3.76–3.70 (m, 1H), 3.73 (s, 3H), 3.41–3.39 (m, *J* = 7.2 Hz, 1H), 2.27–2.15 (m, 2H), 2.03–1.94 (m, 2H); ^{13}C{^{1}H} NMR ($CDCl_3$, 125 MHz) δ 172.9, 169.9, 156.2, 136.2, 128.5 (2C), 128.1, 128.0 (2C), 67.0, 63.8, 58.9, 53.8, 52.7, 47.3, 28.9, 24.8; IR (film) υ_{max} 3315, 2953, 2348, 1720, 1639, 1529, 1449, 1216, 1061 cm^{-1}; HRMS (ESI-TOF) *m/z*: $[M + H]^+$ Calcd for $C_{17}H_{22}N_2O_6H$ 351.1556; Found 351.1549.

Methyl (2-(((Benzyloxy)carbonyl)amino)acryloyl)-l-prolinate (10).

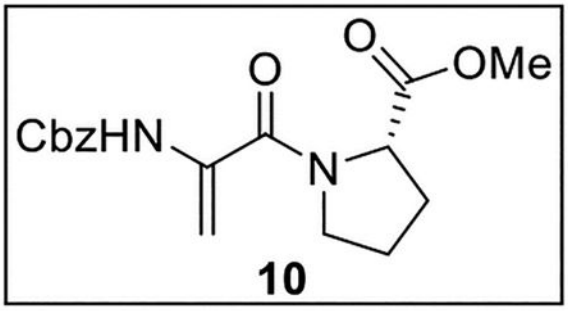

A solution of **9** (380.7 mg, 1.09 mmol) in 1,2-dichloroethane (15 mL) at 0 °C was treated with Et_3N (380 μL, 276 mg, 2.73 mmol, 2.5 equiv), then stirred at 0 °C for 10 min. The resulting mixture was treated dropwise with MsCl (170 μL, 252 mg, 2.20 mmol, 2.0 equiv) and stirred at 0 °C to rt for 1 h. It was then treated with DBU (810 μL, 825 mg, 5.42 mmol, 5.0 equiv) and stirred at 90 °C for 2 h. The mixture was concentrated *in vacuo*, and the residue was dissolved in EtOAc (15 mL) and washed with 10% aq citric acid (10 mL), sat aq $NaHCO_3$ (2 × 8 mL), and brine (10 mL). The combined organic layers were dried (Na_2SO_4)

and concentrated *in vacuo*. Flash chromatography (110 mL of SiO_2, 0–13% MeOH in CH_2Cl_2 gradient elution) afforded **10** (223.2 mg, 0.672 mmol, 62%) as a white solid: $[\alpha]^{25}_D$ −43 (*c* 0.6, $CHCl_3$); ^1H NMR ($CDCl_3$, 500 MHz) δ 7.38–7.30 (m, 5H), 7.23 (br s, 1H), 6.13 (s, 1H), 5.14 (s, 3H), 4.55–4.48 (m, 1H), 3.83–3.77 (m, 2H), 3.74 (s, 3H), 2.30–2.21 (m, 1H), 2.10–2.01 (m, 1H), 2.00–1.84 (m, 2H); $^{13}C\{^1H\}$ NMR ($CDCl_3$, 125 MHz) δ 172.3, 165.0, 153.3, 136.0, 134.8, 128.5 (2C), 128.3, 128.1 (2C), 102.6, 66.8, 59.8, 52.3, 50.4, 28.9, 25.4; IR (film) υ_{max} 3303, 2953, 2881, 1738, 1622, 1511, 1438, 1219, 1088 cm^{-1}; HRMS (ESI-TOF) *m/z*: $[M + H]^+$ Calcd for $C_{17}H_{20}N_2O_5H$ 333.1445; Found 333.1438.

Methyl (2-(1-(2-(((Benzyloxy)carbonyl)amino)acryloyl)pyrrolidine-2-carboxamido)-2-methylpropanoyl)-l-alaninate (2b).

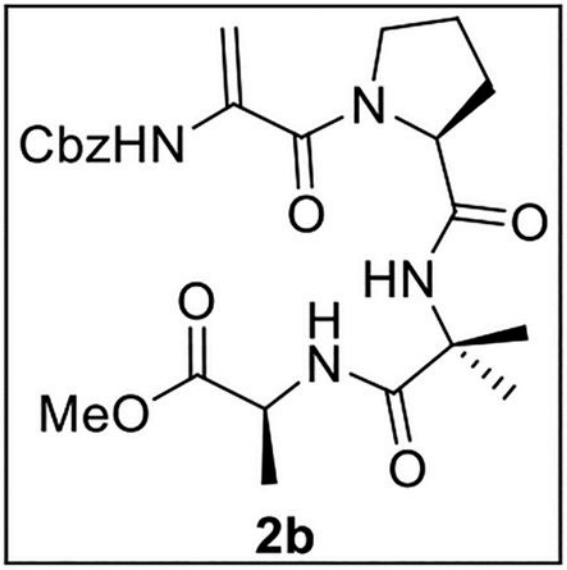

2b

A solution of **10** (150.6 mg, 0.453 mmol) in *t*-BuOH–H_2O (3:1, 10 mL) at 0 °C was treated with $LiOH{\cdot}H_2O$ (95.1 mg, 2.27 mmol, 5.0 equiv) and stirred at rt for 4 h. The reaction was quenched by the addition of 1N HCl until pH ~4, and the mixture was extracted with EtOAc (4 × 10 mL). The combined organic layers were washed with brine (10 mL), dried (Na_2SO_4), and concentrated *in vacuo*. Crude acid Z-ΔAla-Pro-OH (105.2 mg, 0.330 mmol, 73%) was obtained as a colorless oil and was used in subsequent reactions without further purification.

A solution of Z-ΔAla-Pro-OH (105 mg, 0.330 mmol) in anhydrous THF–DMF (5:1, 18 mL) at 0 °C under Ar was treated sequentially with Aib-Ala-OMe (**4**, 65.2 mg, 0.346 mmol, 1.05 equiv), HOBt (ca. 20% H_2O content, 71.7 mg, 0.425 mmol, 1.3 equiv), EDC·HCl (88.5 mg, 0.462 mmol, 1.4 equiv), and $NaHCO_3$ (66.5 mg, 0.792 mmol, 2.4 equiv). The resulting mixture was slowly warmed to rt and stirred for 24 h. The reaction was quenched by the addition of sat aq $NaHCO_3$ (5 mL), diluted with H_2O (5 mL), and extracted with EtOAc (4 × 8 mL). The combined organic layers were dried (Na_2SO_4) and concentrated *in vacuo*. Flash chromatography (60 mL of SiO_2, 0–3% MeOH in CH_2Cl_2 gradient elution) afforded **2b** (93.7 mg, 0.192 mmol, 58%, 42% from **10**) as a white solid: $[\alpha]^{25}_D$ −14 (*c* 0.5, $CHCl_3$); ^1H NMR ($CDCl_3$, 500 MHz) δ 7.40–7.31 (m, 5H), 7.27 (br s, 1H), 7.17 (br s, 1H), 6.96 (br s,

1H), 5.60 (s, 1H), 5.15 (d, J = 12.3 Hz, 1H), 5.12 (d, J = 12.4 Hz, 1H), 5.01 (s, 1H), 4.51 (quint, J = 7.2 Hz, 1H), 4.42–4.36 (m, 1H), 3.75–3.67 (m, 2H), 3.66 (s, 3H), 2.22–2.12 (m, 2H), 2.11–2.03 (m, 1H), 1.93–1.86 (m, 1H), 1.56 (s, 3H), 1.52 (s, 3H), 1.33 (d, J = 7.2 Hz, 3H); $^{13}C\{^{1}H\}$ NMR ($CDCl_3$, 125 MHz) δ 174.0, 173.6, 170.7, 165.7, 153.4, 135.8, 135.6, 128.6 (2C), 128.5, 128.2 (2C), 102.6, 67.4, 61.7, 57.3, 52.2, 50.2, 48.3, 28.7, 26.3, 25.3, 24.6, 17.7; IR (film) υ_{max} 3324, 2951, 1715, 1649, 1523, 1450, 1243, 1090 cm^{-1}; HRMS (ESI-TOF) m/z: $[M + H]^+$ Calcd for $C_{24}H_{32}N_4O_7H$ 489.2349; Found 489.2357.

((Benzyloxy)carbonyl)-l-threonyl-l-proline (11).

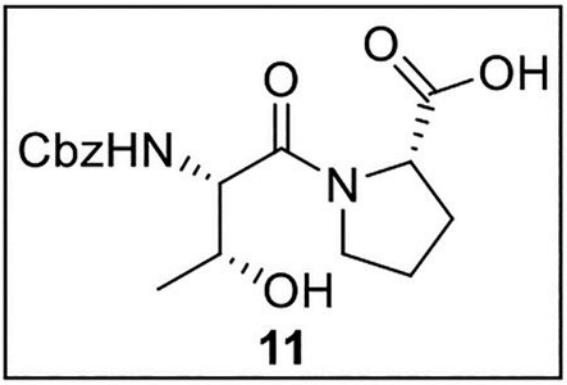

11

A solution of Z-Thr-OH (1.004 g, 3.96 mmol) in anhydrous THF–DMF (5:1, 24 mL) under Ar at 0 °C was treated sequentially with Pro-OMe·HCl (707 mg, 4.27 mmol, 1.1 equiv), HOBt (ca. 20% H_2O content, 811.5 mg, 4.80 mmol, 1.2 equiv), EDC·HCl (1.085 g, 5.66 mmol, 1.4 equiv), and $NaHCO_3$ (798.1 mg, 9.50 mmol, 2.4 equiv). The resulting mixture was allowed to warm to rt and was stirred for 24 h. The reaction was quenched by the addition of sat aq $NaHCO_3$ (25 mL), diluted with H_2O (30 mL), and extracted with EtOAc (5 × 40 mL). The combined organic layers were dried (Na_2SO_4) and concentrated *in vacuo*. Flash chromatography (200 mL of SiO_2, 0–30% EtOAc in hexanes gradient elution) afforded Z-Thr-Pro-OMe (1.3584 g, 3.73 mmol, 94%) as a white solid: $[\alpha]^{25}_D$ −88 (c 0.49, $CHCl_3$); ^1H NMR ($CDCl_3$, 500 MHz) δ 7.40–7.31 (m, 5H), 5.70 (d, J = 9.0 Hz, 1H), 5.14 (d, J = 12.2 Hz, 1H), 5.10 (d, J = 12.4 Hz, 1H), 4.57–4.53 (m, 1H), 4.48 (dd, J = 9.2, 2.0 Hz, 1H), 4.24–4.17 (m, 1H), 3.86–3.80 (m, 1H), 3.78–3.73 (m, 1H), 3.75 (s, 3H), 3.38 (br s, 1H), 2.30–2.21 (m, 1H), 2.10–1.97 (m, 3H), 1.24 (d, J = 6.4 Hz, 3H); $^{13}C\{^{1}H\}$ NMR ($CDCl_3$, 125 MHz) δ 172.5, 170.6, 156.6, 136.2, 128.5 (2C), 128.2, 128.0 (2C), 67.3, 67.1, 58.8, 56.0, 52.5, 47.3, 28.9, 24.9, 18.5; IR (film) υ_{max} 3399, 2977, 1744, 1720, 1634, 1524, 1439, 1218, 1176, 1027 cm^{-1}; HRMS (ESI-TOF) m/z: $[M + H]^+$ Calcd for $C_{18}H_{24}N_2O_6H$ 365.17126; Found 365.17005.

A solution of Z-Thr-Pro-OMe (800.0 mg, 2.20 mmol) in t-BuOH–H_2O (3:1, 12 mL) at 0 °C was treated with $LiOH·H_2O$ (480.5 mg, 11.45 mmol, 5.2 equiv) and stirred for 4 h. The reaction was quenched by the addition of 1 N HCl until pH ~2, and the mixture was extracted with EtOAc (4 × 15 mL). The combined organic layers were washed with brine (10 mL), dried (Na_2SO_4), and concentrated *in vacuo*. Crude acid **11** (616.7 mg, 1.76 mmol, 80%) was obtained as a colorless oil and was used in subsequent reactions without further purification.

Methyl (2-((*S*)-1-(((Benzyloxy)carbonyl)-l-threonyl)pyrrolidine-2-carboxamido)-2-methylpropanoyl)-l-alaninate (12).

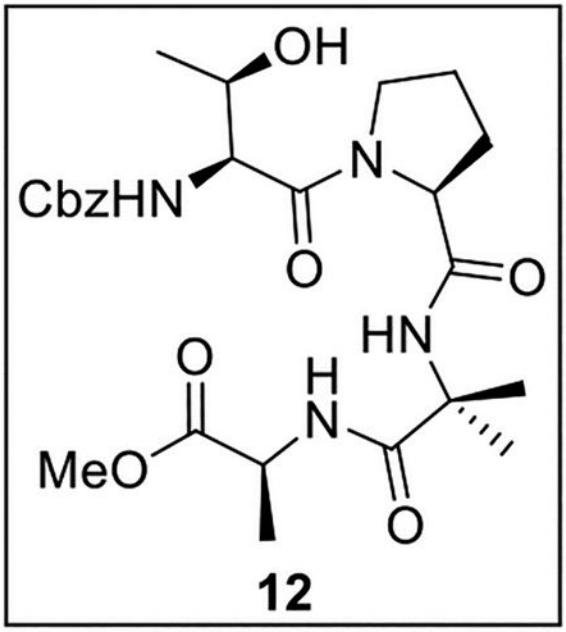

A solution of acid **11** (240.4 mg, 0.686 mmol) in anhydrous DMF (10 mL) at 0 °C under Ar was treated sequentially with HBTU (262.3 mg, 0.692 mmol, 1.0 equiv), *i*-Pr_2NEt (360 μL, 267 mg, 2.07 mmol, 3.0 equiv), and amine **4** (159.9 mg, 0.850 mmol, 1.2 equiv). The resulting mixture was warmed to rt and stirred for 2 h, then diluted with EtOAc (15 mL) and washed with sat aq NH_4Cl (3 × 15 mL), sat aq $NaHCO_3$ (2 × 15 mL), and brine (15 mL). The organic layer was dried (Na_2SO_4) and concentrated *in vacuo*. Flash chromatography (100 mL of SiO_2, 2–4.5% MeOH in CH_2Cl_2 gradient elution) afforded **12** (89.5 mg, 0.172 mmol, 25%) as a white solid: $[\alpha]^{25}_D$ −34 (*c* 0.34, $CHCl_3$); ^1H NMR ($CDCl_3$, 500 MHz) δ 7.37–7.32 (m, 6H), 7.00 (br s, 1H), 6.94 (d, *J* = 7.0 Hz, 1H), 5.75 (d, *J* = 8.7 Hz, 1H), 5.14 (d, *J* = 12.2 Hz, 1H), 5.10 (d, *J* = 12.2 Hz, 1H), 4.56–4.52 (m, 2H), 4.50–4.48 (m, 1H), 4.26–4.21 (m, 1H), 3.74 (s, 3H), 3.73–3.70 (m, 2H), 2.27–2.18 (m, 1H), 2.13–2.07 (m, 1H), 2.06–1.96 (m, 2H), 1.59 (s, 3H), 1.46 (s, 3H), 1.37 (d, *J* = 7.2 Hz, 3H), 1.26 (d, *J* = 4.0 Hz, 3H); $^{13}C\{^1H\}$ NMR ($CDCl_3$, 125 MHz) δ 173.9, 173.8, 171.1, 170.7, 156.6, 136.2, 128.5 (2C), 128.2, 128.0 (2C), 67.2, 67.1, 60.5, 57.1, 56.5, 52.5, 48.3, 47.7, 27.3, 26.8, 25.2, 23.9, 19.0, 18.1; IR (film) υ_{max} 3312, 2923, 1735, 1633, 1529, 1454, 1256 cm^{-1}; HRMS (ESI-TOF) *m*/*z*: $[M + H]^+$ Calcd for $C_{25}H_{36}N_4O_8H$ 521.2611; Found 521.2602.

Methyl (2-((*S*)-1-((*Z*)-2-(((Benzyloxy)carbonyl)amino)but-2-enoyl)pyrrolidine-2-carboxamido)-2-methylpropanoyl)-l-alaninate (2c).

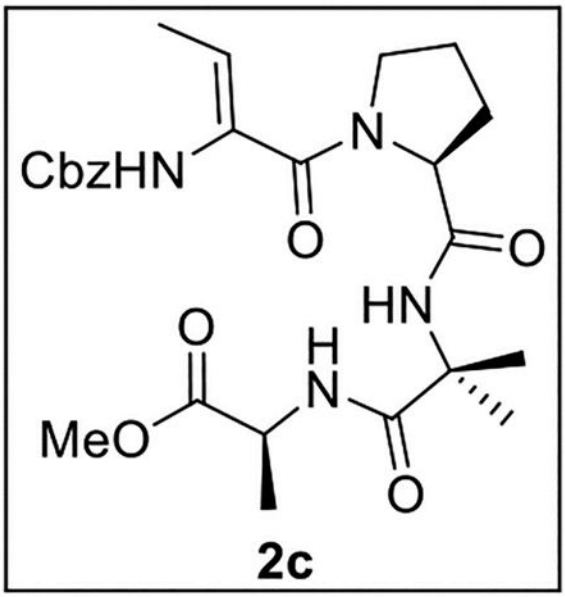

A solution of tetrapeptide **12** (55.0 mg, 0.106 mmol) in anhydrous $CHCl_3$ (3 mL) at 0 °C was treated with Martin sulfurane (152 mg, 0.226 mmol, 2.1 equiv). The resulting mixture was stirred at 0 °C to rt for 1 h, dried (Na_2SO_4), and concentrated *in vacuo*. Flash chromatography (150 mL of SiO_2, 2–4.5% MeOH in CH_2Cl_2 gradient elution) afforded **2c** (23.1 mg, 0.0460 mmol, 44%) as a white film: $[\alpha]^{25}_D$ −32 (*c* 0.85, $CHCl_3$); ^{1}H NMR ($CDCl_3$, 500 MHz) δ 7.40–7.31 (m, 7H), 6.49 (br s, 1H), 5.52 (q, *J* = 6.8 Hz, 1H), 5.16 (d, *J* = 12.1 Hz, 1H), 5.10 (d, *J* = 12.1 Hz, 1H), 4.54–4.45 (m, 2H), 3.70 (s, 3H), 3.63–3.50 (m, 2H), 2.24–2.12 (m, 2H), 1.98–1.85 (m, 2H), 1.73 (d, *J* = 7.0 Hz, 3H), 1.55 (s, 3H), 1.53 (s, 3H), 1.37 (d, *J* = 7.2 Hz, 3H);^{13}C{^{1}H} NMR ($CDCl_3$, 125 MHz) δ 174.4, 173.5, 170.6, 166.6, 153.7, 135.4, 130.7, 128.7 (2C), 128.6, 128.3 (2C), 117.1, 67.8, 61.4, 57.3, 52.1, 49.6, 48.3, 29.0, 25.6, 25.4, 24.9, 17.6, 11.7; IR (film) υ_{max} 3320, 2924, 2359, 1669, 1521, 1456, 1255 cm^{-1}; HRMS (ESI-TOF) *m*/*z*: $[M + H]^+$ Calcd for $C_{25}H_{34}N_4O_7H$ 503.2506; Found 503.2513.

(2-(((Benzyloxy)carbonyl)amino)-2-methylpropanoyl)-l-proline (13).

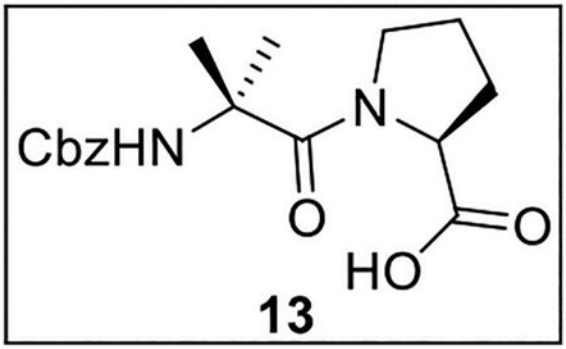

A solution of Z-Aib-OH (750.6 mg, 3.16 mmol) in anhydrous THF–DMF (5:1, 24 mL) at 0 °C under Ar was treated sequentially with Pro-OMe·HCl (557.6 mg, 3.37 mmol, 1.1 equiv), HOBt (ca. 20% H_2O content, 645.1 mg, 3.82 mmol, 1.2 equiv), EDC·HCl (861.2 mg, 4.49 mmol, 1.4 equiv), and $NaHCO_3$ (641.7 mg, 7.64 mmol, 2.4 equiv). The resulting mixture was allowed to warm to rt and was stirred for 24 h. The reaction was quenched by the addition of sat aq $NaHCO_3$ (15 mL), diluted with H_2O (30 mL), and extracted with EtOAc (5 × 30 mL). The combined organic layers were dried (Na_2SO_4) and concentrated *in vacuo*. Flash chromatography (150 mL of SiO_2, 0–30% EtOAc in hexanes gradient elution) afforded Z-Aib-Pro-OMe (750.7 mg, 2.15 mmol, 68%) as a white solid: $[\alpha]^{25}_D$ −52 (*c* 2.64, $CHCl_3$); ^{1}H NMR ($CDCl_3$, 500 MHz) δ 7.36–7.29 (m, 5H), 5.65 (br s, 1H), 5.11 (d, *J* = 11.8 Hz, 1H), 5.03 (d, *J* = 11.6 Hz, 1H), 4.58–4.52 (m, 1H), 3.70 (s, 3H), 3.50–3.42 (m, 1H), 3.38–3.29 (m, 1H), 2.08–1.94 (m, 2H), 1.91–1.80 (m, 2H), 1.59 (s, 3H), 1.54 (s, 3H); $^{13}C\{^1H\}$ NMR ($CDCl_3$, 125 MHz) δ 173.0, 172.1, 154.2, 136.6, 128.4 (2C), 128.2, 128.1 (2C), 66.4, 60.8, 56.7, 52.1, 47.9, 27.7, 25.8, 24.7, 24.3; IR (film) υ_{max} 3303, 2986, 1720, 1623, 1525, 1411, 1364, 1258, 1168, 1074 cm^{-1}; HRMS (ESI-TOF) *m/z*: $[M + H]^+$ Calcd for $C_{18}H_{24}N_2O_5H$ 349.1763; Found 349.1757.

A solution of Z-Aib-Pro-OMe (56.2 mg, 0.161 mmol) in *t*-BuOH (1.0 mL) and H_2O (0.4 mL) was treated with $LiOH·H_2O$ (34.1 mg, 0.813 mmol, 5.0 equiv), then stirred at rt for 4 h. The resulting mixture was acidified to pH 4~5 by the addition of 1 N HCl, diluted with H_2O (2 mL), and extracted with EtOAc (3 × 5 mL). The combined organic layers were dried (Na_2SO_4) and concentrated *in vacuo*. The crude carboxylic acid **13** was used directly in subsequent coupling reactions without further purification.

Ethyl (*S*)-2-((*S*)-1-(2-(((Benzyloxy)carbonyl)amino)-2-methylpropanoyl)pyrrolidine-2-carboxamido)-3-hydroxy-3-methylbutanoate (15).

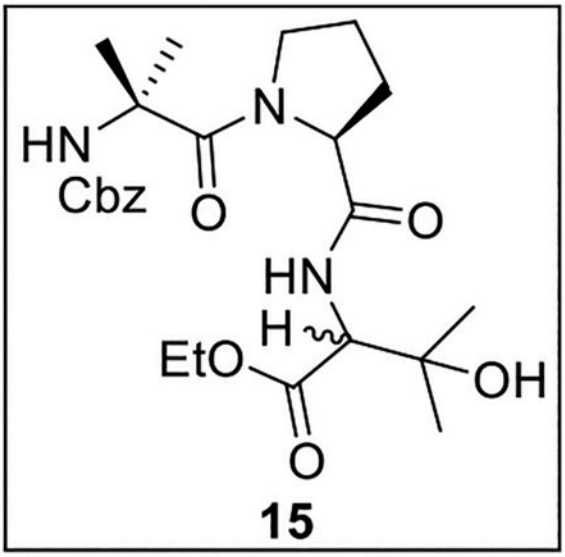

15

A solution of **13** (506.8 mg, 1.52 mmol) in anhydrous THF–DMF (5:1, 12 mL) at 0 °C under Ar was treated with **14**[32] (248.4 mg, 1.54 mmol, 1.0 equiv), HOBt (ca. 20% H_2O content, 322.3 mg, 1.91 mmol, 1.3 equiv), EDC·HCl (413.5 mg, 2.16 mmol, 1.4 equiv), and $NaHCO_3$

(314.0 mg, 3.74 mmol, 2.5 equiv). The resulting mixture was warmed to rt and stirred for 24 h. The reaction was quenched by the addition of sat aq $NaHCO_3$ (15 mL), diluted with H_2O (30 mL), and extracted with EtOAc (5 × 40 mL). The combined organic layers were dried (Na_2SO_4) and concentrated *in vacuo*. Flash chromatography (150 mL of SiO_2, 0–60% EtOAc in hexanes gradient elution) afforded **15** (558.4 mg, 1.17 mmol, 77%) as a colorless oil that was a 1:1 mixture of diastereomers: ^1H NMR ($CDCl_3$, 500 MHz) δ 7.68–7.60 (m, 1H), 7.42–7.32 (m, 5H), 5.22–5.02 (m, 3H), 4.70–4.55 (m, 1H), 4.40–4.15 (m, 3H), 4.06 and 3.85 (2 br s, 1H), 3.72–3.60 (m, 1H), 3.467–3.35 (m, 1H), 2.21–2.12 (m, 1H), 2.02–1.80 (m, 3H), 1.61 (s, 6H), 1.48 and 1.45 (2s, 3H), 1.44 and 1.36 (2s, 3H), 1.33–1.29 (m, 3H); $^{13}C\{^1H\}$ NMR ($CDCl_3$, 125 MHz) δ 172.4, 171.6 and 171.5, 170.7, 155.7 and 154.9, 135.8 and 135.4, 128.9 and 128.7 (2C), 128.6, 128.5 (2C), 72.2 and 71.9, 68.2, 67.3, 63.0 and 62.2, 61.0 and 60.6, 57.2, 48.2 and 48.0, 28.8, 27.6, 27.1 and 26.6, 26.3 and 26.2, 25.7, 24.7, 14.2; IR (film) υ_{max} 3294, 2980, 1725, 1651, 1536, 1456, 1400, 1274, 1196, 1089 cm^{-1}; HRMS (ESI-TOF) *m*/*z*: $[M + H]^+$ Calcd for $C_{24}H_{35}N_3O_7H$ 478.2553; Found 478.2546.

Methyl (2-((*S*)-1-(2-(((Benzyloxy)carbonyl)amino)-2-methylpropanoyl)pyrrolidine-2-carboxamido)-3-methylbut-2-enoyl)-l-alaninate (3a).

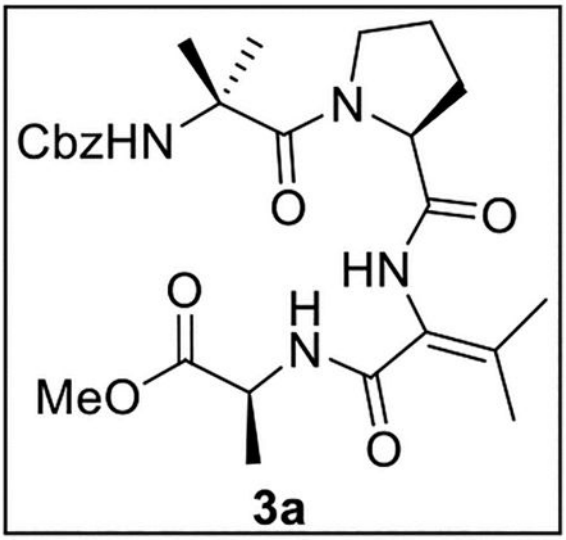

3a

A solution of tripeptide **15** (75.8 mg, 0.159 mmol) in *t*-BuOH–H_2O (3:1, 8 mL), was treated with $LiOH·H_2O$ (36.0 mg, 0.858 mmol, 5.4 equiv). The mixture was stirred at rt for 4 h, and the reaction was quenched by the addition of 1N HCl until pH ~2. The mixture was then extracted with EtOAc (4 × 15 mL), and the combined organic layers were washed with brine (10 mL), dried (Na_2SO_4), and concentrated *in vacuo*. The crude acid was then dissolved in anhydrous THF (8 mL) and treated with NaOAc (19.3 mg, 0.235 mmol, 1.5 equiv) and Ac_2O (75 μL, 81.2 mg, 0.795 mmol, 5.0 equiv). The resulting mixture was stirred at rt under Ar for 12 h, then diluted with MeOH (10 mL), stirred for an additional 30 min, and diluted with H_2O (10 mL). The mixture was extracted with EtOAc (4 × 15 mL), and the combined organic layers were washed with brine (10 mL), dried (Na_2SO_4), and concentrated *in vacuo*.

The crude azlactone (40.2 mg, 0.0972 mmol) was then dissolved in MeOH (2 mL) and treated dropwise with 1 N NaOH (970 μL, 0.97 mmol, 10 equiv). The resulting mixture was stirred at rt for 24 h, then washed with sat aq $NaHCO_3$ (2 × 5 mL) and acidified by the addition of 1 N HCl to pH ~2. The mixture was extracted with EtOAc (3 × 5 mL), and the combined organic layers were dried (Na_2SO_4) and concentrated *in vacuo*. The crude *C*-terminal dehydroamino acid was dissolved in anhydrous THF–DMF (5:1, 3 mL) and treated sequentially with Ala-OMe (42.6 mg, 0.305 mmol, 3.1 equiv), PyBOP (152.4 mg, 0.293 mmol, 3.0 equiv), and *i*-Pr_2NEt (100 μL, 74.2 mg, 0.574 mmol, 3.6 equiv). The resulting mixture was stirred at rt under Ar for 24 h, then extracted with EtOAc (5 × 5 mL). The combined organic layers were dried (Na_2SO_4) and concentrated *in vacuo*. Flash chromatography (25 mL of SiO_2, 2–4.5% MeOH in CH_2Cl_2 gradient elution) afforded **3a** (17.0 mg, 0.0329 mmol, 34% from azlactone and 21% from **15**) as a white film: $[\alpha]^{25}_D$ +12.7 (*c* 0.41, $CHCl_3$); ^1H NMR ($CDCl_3$, 500 MHz) δ 8.14 (s, 1H), 7.39–7.30 (m, 6H), 5.30 (s, 1H), 5.16 (d, *J* = 12.1 Hz, 1H), 4.96 (d, *J* = 12.1 Hz, 1H), 4.59–4.51 (m, 2H), 3.71 (s, 3H), 3.70–3.65 (m, 1H), 3.26–3.19 (m, 1H), 2.30–2.23 (m, 1H), 2.23 (s, 3H), 1.90–1.78 (m, 3H), 1.78 (s, 3H), 1.55 (s, 3H) 1.46 (d, *J* = 7.2 Hz, 3H), 1.44 (s, 3H); $^{13}C\{^1H\}$ NMR ($CDCl_3$, 125 MHz) δ 173.5, 172.4, 171.0, 165.4, 155.3, 144.6, 136.0, 128.6 (2C), 128.5, 128.4 (2C), 122.3, 67.3, 63.2, 57.0, 52.1, 48.5, 48.3, 28.7, 26.5, 26.0, 24.6, 22.1, 21.1, 17.6; IR (film) υ_{max} 3306, 2987, 1666, 1625, 1535, 1454, 1273, 1077 cm^{-1}; HRMS (ESI-TOF) *m*/*z*: $[M + H]^+$ Calcd for $C_{26}H_{36}N_4O_7H$ 517.2662; Found 517.2670.

Methyl ((Benzyloxy)carbonyl)-l-seryl-l-alaninate (16).

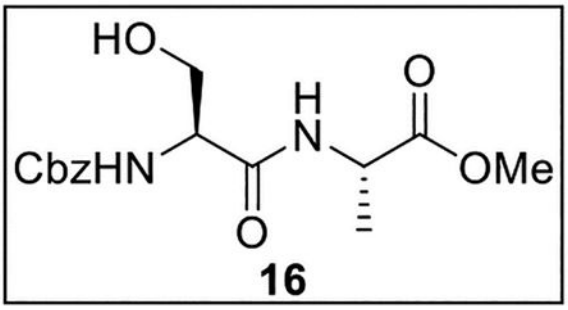

16

A solution of Z-Ser-OH (500.2 mg, 2.09 mmol) in anhydrous THF–DMF (5:1, 18 mL) under Ar at 0 °C was treated sequentially with Ala-OMe·HCl (291.7 mg, 2.09 mmol, 1.0 equiv), HOBt (ca. 20% H_2O content, 423.6 mg, 2.51 mmol, 1.2 equiv), EDC·HCl (520.8 mg, 2.72 mmol, 1.3 equiv), and $NaHCO_3$ (403.8 mg, 4.81 mmol, 2.3 equiv). The resulting mixture was slowly warmed to rt and stirred for 24 h. The reaction was quenched by the addition of sat aq $NaHCO_3$ (20 mL), diluted with H_2O (25 mL), and extracted with EtOAc (4 × 25 mL). The combined organic layers were dried (Na_2SO_4) and concentrated *in vacuo*. Flash chromatography (170 mL of SiO_2, 0–5% MeOH in DCM gradient elution) afforded **16** (489.3 mg, 1.51 mmol, 72%) as a white solid: $[\alpha]^{25}_D$ −11 (*c* 0.6, $CHCl_3$); ^1H NMR ($CDCl_3$, 500 MHz) δ 7.39–7.31 (m, 5H), 7.13–7.01 (m, 1H), 5.92–5.83 (m, 1H), 5.13 (s, 2H), 5.10 (br s, 1H), 4.57 (quint, *J* = 7.3 Hz, 1H), 4.33–4.28 (m, 1H), 4.08–4.00 (m, 1H), 3.76 (s, 3H), 3.68 (dd, *J* = 11.2, 6.2 Hz, 1H), 1.41 (d, *J* = 7.1 Hz, 3H); $^{13}C\{^1H\}$ NMR ($CDCl_3$, 125 MHz) δ 173.4, 170.6, 156.5, 136.0, 128.6 (2C), 128.3, 128.1 (2C), 67.3, 63.0, 55.4, 52.7, 48.3,

17.7; IR (film) υ_{max} 3314, 1736, 1665, 1562, 1547, 1460, 1217, 1058 cm^{-1}; HRMS (ESI-TOF) *m*/*z*: $[M + H]^+$ Calcd for $C_{15}H_{20}N_2O_6H$ 325.1400; Found 325.1408.

Methyl (2-(((Benzyloxy)carbonyl)amino)-2-methylpropanoyl)-l-prolyl-l-seryl-l-alaninate (17).

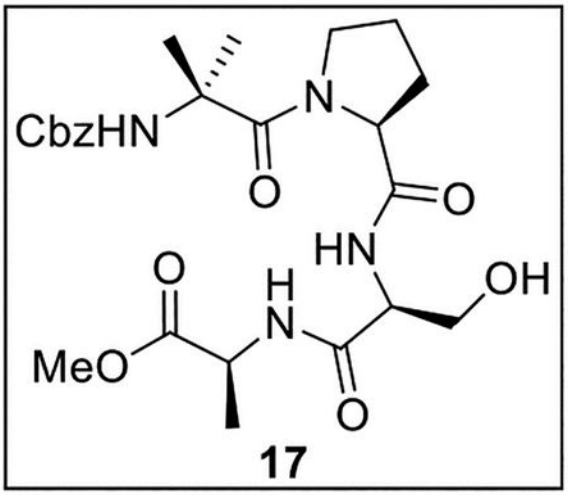

A solution of **16** (106.7 mg, 0.329 mmol) in MeOH (6.0 mL) was treated with 10% Pd/C (70.2 mg, 0.66 wt equiv) at rt under Ar. The resulting mixture was stirred at rt under H_2 (500 psi) for 48 h, then diluted with H_2O (10 mL) and extracted with EtOAc (4 × 6 mL). The combined organic layers were dried (Na_2SO_4) and concentrated *in vacuo*. The crude Ser-Ala-OMe (54.4 mg, 0.286 mmol, 87%) was used directly in subsequent couplings without further purification.

A solution of crude carboxylic acid **13** (94.6 mg, 0.283 mmol) in anhydrous DMF (3.0 mL) at 0 °C under Ar was treated with HBTU (107.4 mg, 0.282 mmol, 1.0 equiv) and *i*-Pr_2NEt (51.0 μL, 37.8 mg, 0.293 mmol, 1.0 equiv). The resulting mixture was treated dropwise with a solution of Ser-Ala-OMe (54.4 mg, 0.286 mmol, 1.0 equiv) in anhydrous DMF (1 mL) and stirred at 0 °C under Ar for 2 h. It was then diluted with H_2O (8 mL) and extracted with EtOAc (3 × 10 mL). The combined organic layers were washed with sat aq NH_4Cl (3 × 5 mL), sat aq $NaHCO_3$ (2 × 4 mL), and brine (6 mL), dried (Na_2SO_4), and concentrated *in vacuo*. Flash chromatography (110 mL of SiO_2, 0–10% MeOH in CH_2Cl_2 gradient elution) afforded **17** (61.6 mg, 0.122 mmol, 37% from **16**) as a white solid: $[\alpha]^{25}_D$ + 22 (*c* 0.6, $CHCl_3$); ^1H NMR ($CDCl_3$, 500 MHz, ca. 1.2:1 mixture of rotamers) δ 7.63 and 7.57 (2d, *J* = 8.8 Hz and *J* = 7.4 Hz, 1H), 7.38–7.32 (m, 5H), 7.21 (br s, 1H), 5.75 (br s, 1H), 5.34 (br s, 1H), 5.23–5.19 and 5.17 (m and d, *J* = 11.8 Hz, 1H), 5.00 and 4.99 (2d, *J* = 12.2 and 12.1 Hz, 1H), 4.60–4.50 (m, 2H), 4.06–4.00 (m, 1H), 3.83 (dd, *J* = 11.4, 4.7 Hz, 1H), 3.71 (s, 3H), 3.67–3.60 (m, 1H), 3.18–3.09 (m, 2H), 2.33–2.27 (m, 1H), 2.17–2.10 and 1.92–1.85 (2m, 1H), 1.80–1.70 (m, 2H), 1.59 and 1.54 (2s, 3H), 1.46 (d, *J* = 7.4 Hz, 3H) 1.45 and 1.42 (2s, 3H); $^{13}C\{^1H\}$ NMR ($CDCl_3$, 125 MHz) δ 174.9, 172.9 and 172.8, 171.4, 170.9, 155.9 and 155.3, 135.9 and 135.6, 128.7 (2C), 128.6, 128.3 (2C), 67.7 and 67.3, 63.3 and 63.0, 62.4, 57.2, 54.7, 52.3, 48.7, 48.3 and 48.1, 28.6 and 28.5, 26.7 and 26.5, 26.0 and 25.7, 24.7 and 24.3, 17.4; IR (film) υ_{max} 3306, 2987, 1666, 1625, 1535, 1454, 1273, 1077 cm^{-1}; HRMS (ESI-TOF) *m*/*z*: $[M + H]^+$ Calcd for $C_{24}H_{34}N_4O_8H$ 507.2455; Found 507.2461.

Methyl (2-((*S*)-1-(2-(((Benzyloxy)carbonyl)amino)-2-methylpropanoyl)pyrrolidine-2-carboxamido)acryloyl)-l-alaninate (3b).

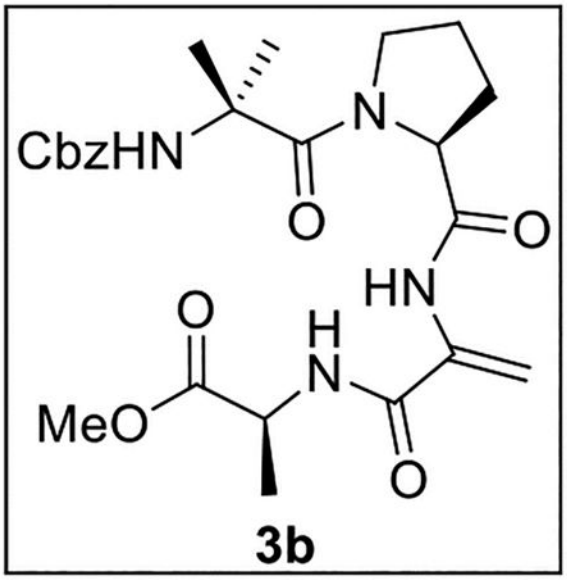

A solution of **17** (40.4 mg, 0.0798 mmol) in 1,2-dichloroethane (6 mL) at 0 °C was treated with Et_3N (28 μL, 20.3 mg, 0.20 mmol, 2.5 equiv), then stirred at 0 °C for 10 min. The resulting mixture was treated dropwise with MsCl (12 μL, 17.8 mg, 0.155 mmol, 1.9 equiv), warmed to rt, and stirred for 1 h. It was then treated with DBU (60 μL, 61.1 mg, 0.401 mmol, 5.0 equiv) and stirred at 90 °C for 16 h. The mixture was concentrated *in vacuo*, and the residue was dissolved in EtOAc (10 mL) and washed with 10% aq citric acid (6 mL), sat aq $NaHCO_3$ (2 × 5 mL), and brine (10 mL). The combined organic layers were dried (Na_2SO_4) and concentrated *in vacuo*. Flash chromatography (50 mL of SiO_2, 0–10% MeOH in CH_2Cl_2 gradient elution) afforded **3b** (14.2 mg, 0.0291 mmol, 36%) as a white solid: $[\alpha]^{25}_D$ +6.1 (*c* 0.6, $CHCl_3$); ^1H NMR ($CDCl_3$, 500 MHz) δ 8.45 (s, 1H), 7.42–7.30 (m, 5H), 7.10 (br s, 1H), 5.90 (s, 1H), 5.88 (s, 1H), 5.29 (s, 1H), 5.13 (d, *J* = 11.6 Hz, 1H), 5.00 (d, *J* = 12.0 Hz, 1H), 4.63 (quint, *J* = 7.1 Hz, 1H), 4.59–4.53 (m, 1H), 3.76 (s, 3H), 3.62–3.55 (m, 1H), 3.30–3.22 (m, 1H), 2.17–2.09 (m, 1H), 1.96–1.90 (m, 1H), 1.88–1.75 (m, 2H), 1.57 (s, 3H), 1.50 (s, 3H), 1.46 (d, *J* = 7.2 Hz, 3H); $^{13}C\{^1H\}$ NMR ($CDCl_3$, 125 MHz) δ 176.7, 173.0, 172.6, 171.0, 156.0, 136.1, 128.7 (2C), 128.6 (2C), 128.5, 128.1, 111.9, 67.2, 66.9, 63.2, 57.0, 52.5, 48.6, 29.4, 26.7, 26.0, 24.6, 18.0; IR (film) υ_{max} 3301, 2950, 1668, 1532, 1455, 1263, 1170, 1075 cm^{-1}; HRMS (ESI-TOF) *m*/*z*: $[M + H]^+$ Calcd for $C_{24}H_{32}N_4O_7H$ 489.2349; Found 489.2357.

Methyl l-Threonyl-l-alaninate (18).

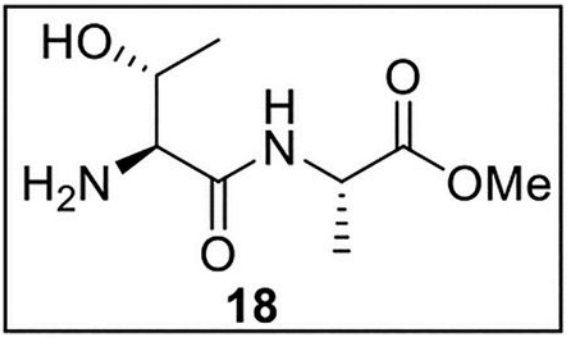

A solution of Z-Thr-OH (1.0021 g, 3.96 mmol) in anhydrous THF–DMF (5:1, 24 mL) under Ar at 0 °C was treated sequentially with Ala-OMe·HCl (594.0 mg, 4.26 mmol, 1.1 equiv), HOBt (ca. 20% H_2O content, 800.5 mg, 4.74 mmol, 1.2 equiv), EDC·HCl (1.0621 g, 5.54 mmol, 1.4 equiv), and $NaHCO_3$ (801.4 mg, 9.54 mmol, 2.4 equiv). The resulting mixture was allowed to warm to rt and was stirred for 24 h. The reaction was quenched by the addition of sat aq $NaHCO_3$ (25 mL), diluted with H_2O (30 mL), and extracted with EtOAc (5 × 40 mL). The combined organic layers were dried (Na_2SO_4) and concentrated *in vacuo*. Flash chromatography (200 mL of SiO_2, 0–30% EtOAc in hexanes gradient elution) afforded Z-Thr-Ala-OMe (1.2778 g, 3.78 mmol, 95%) as a white solid: $[\alpha]^{25}_D$ −23 (*c* 0.50, $CHCl_3$); ^{1}H NMR ($CDCl_3$, 500 MHz) δ 7.39–7.32 (m, 5H), 6.96 (d, *J* = 6.7 Hz, 1H), 5.77 (d, *J* = 7.6 Hz, 1H), 5.17 (d, *J* = 12.2 Hz, 1H), 5.12 (d, *J* = 12.2 Hz, 1H), 4.56 (quint, *J* = 7.3 Hz, 1H), 4.38–4.32 (m, 1H), 4.19 (dd, *J* = 7.8, 2.0 Hz, 1H), 3.76 (s, 3H), 3.17 (br s, 1H), 1.40 (d, *J* = 7.2 Hz, 3H), 1.20 (d, *J* = 6.5 Hz, 3H); ^{13}C{^{1}H} NMR ($CDCl_3$, 125 MHz) δ 173.1, 170.5, 156.8, 136.0, 128.6 (2C), 128.3, 128.0 (2C), 67.3, 66.9, 58.2, 52.6, 48.1, 18.0, 17.9; IR (film) υ_{max} 3324, 3066, 3035, 2956, 1742, 1661, 1538, 1455, 1384, 1293, 1219, 1150, 1051 cm^{-1}; HRMS (ESI-TOF) *m*/*z*: $[M + H]^+$ Calcd for $C_{16}H_{22}N_2O_6H$ 339.15561; Found 339.15492.

A solution of Z-Thr-Ala-OMe (1.200 g, 3.55 mmol) in MeOH (10.0 mL) was treated with 10% Pd/C (602.5 mg, 0.5 wt equiv) at rt under Ar. The suspension was then pressurized under hydrogen gas (500 psig) and stirred for 72 h. The reaction was filtered through Celite, dried (Na_2SO_4), and concentrated *in vacuo*. Amine **18** (534.1 mg, 2.62 mmol, 74%) was obtained as a white solid and was used in subsequent reactions without further purification.

Methyl (2-(((Benzyloxy)carbonyl)amino)-2-methylpropanoyl)-l-prolyl-l-threonyl-l-alaninate (19).

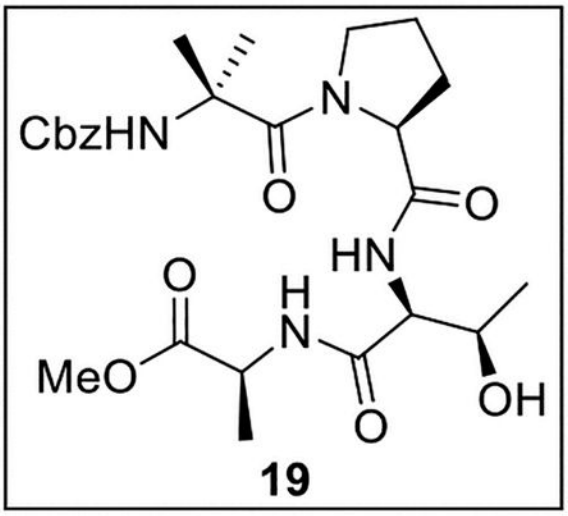

A solution of acid **13** (500.0 mg, 1.50 mmol, 1.0 equiv) in anhydrous THF–DMF (5:1, 12 mL) at 0 °C under Ar was treated with amine **18** (301.1 mg, 1.48 mmol), HOBt (ca. 20% H_2O content, 310.6 mg, 1.84 mmol, 1.2 equiv), EDC·HCl (396.0 mg, 2.07 mmol, 1.4 equiv), and $NaHCO_3$ (304.1 mg, 3.62 mmol, 2.5 equiv). The resulting mixture was warmed to rt, then stirred for 48 h. The reaction was quenched by the addition of sat aq $NaHCO_3$ (15 mL), diluted with H_2O (30 mL), and extracted with EtOAc (5 × 40 mL). The combined organic layers were dried (Na_2SO_4) and concentrated *in vacuo*. Flash chromatography (150 mL of SiO_2, 2–4.5% MeOH in CH_2Cl_2 gradient elution) afforded **19** (167.6 mg, 0.322 mmol, 22%) as a white solid: $[\alpha]^{25}_D$ −8.1 (*c* 0.23, $CHCl_3$); ^{1}H NMR ($CDCl_3$, 500 MHz) δ 7.44 (d, *J* = 9.2 Hz, 1H), 7.40–7.34 (m, 7H), 5.17 (s, 1H), 5.15 (d, *J* = 12.4 Hz, 1H), 5.05 (d, *J* = 12.1 Hz, 1H), 4.61–4.53 (m, 4H), 3.78–3.73 (m, 1H), 3.73 (s, 3H), 3.32–3.27 (m, 1H), 2.36–2.31 (m, 1H), 1.89–1.83 (m, 3H), 1.55 (s, 3H), 1.47–1.44 (m, 3H), 1.46 (s, 3H), 1.21 (d, *J* = 6.4 Hz, 3H); ^{13}C{^{1}H} NMR ($CDCl_3$, 125 MHz) δ 173.0, 172.5, 171.8, 170.6, 155.5, 135.4, 128.7 (2C), 128.7, 128.4 (2C), 67.8, 67.1, 63.5, 58.3, 57.2, 52.2, 48.6, 48.4, 28.9, 26.7, 26.0, 24.6, 19.5, 17.5; IR (film) υ_{max} 3317, 2925, 1744, 1656, 1542, 1454, 1410, 1275, 1211, 1156, 1089 cm^{-1}; HRMS (ESI-TOF) *m*/*z*: [M + H]$^+$ Calcd for $C_{25}H_{36}N_4O_8H^+$ 521.2611; Found 521.2602.

Methyl ((*Z*)-2-((*S*)-1-(2-(((Benzyloxy)carbonyl)amino)-2-methylpropanoyl)pyrrolidine-2-carboxamido)but-2-enoyl)-l-alaninate (3c).

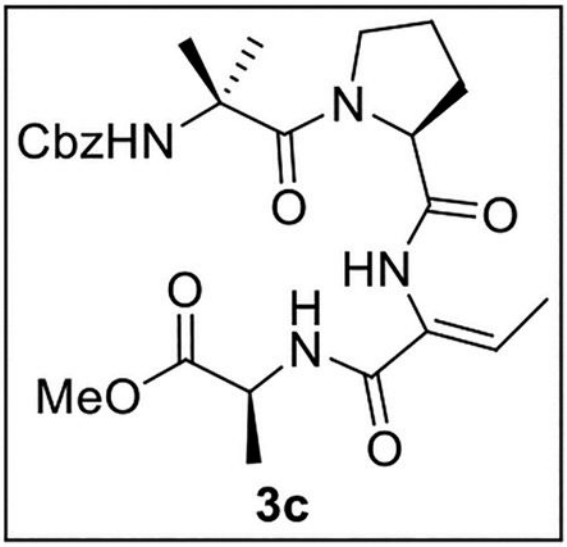

A solution of tetrapeptide **19** (100 mg, 0.192 mmol) in anhydrous $CHCl_3$ (3 mL) at 0 °C was treated with Martin sulfurane (251.1 mg, 0.373 mmol, 1.9 equiv) and stirred at 0 °C to rt for 1 h. The mixture was dried (Na_2SO_4) and concentrated *in vacuo*. Flash chromatography (150 mL of SiO_2, 2–4.5% MeOH in CH_2Cl_2 gradient elution) afforded **3c** (35.0 mg, 0.0696 mmol, 36%) as a white film: $[\alpha]^{25}_D$ +18 (*c* 2.4, $CHCl_3$); ^{1}H NMR ($CDCl_3$, 500 MHz) δ 8.13 (s, 1H), 7.36–7.29 (m, 6H), 6.96 (q, *J* = 7.0 Hz, 1H), 5.41 (s, 1H), 5.16 (d, *J* = 12.1 Hz, 1H), 4.90 (d, *J* = 12.1 Hz, 1H), 4.61 (quint, *J* = 7.2 Hz, 1H), 4.55–4.50 (m, 1H), 3.70 (s, 3H), 3.69–3.65 (m, 1H), 3.18–3.10 (m, 1H), 2.32–2.27 (m, 1H), 1.85–1.74 (m, 3H), 1.72 (d, *J* = 7.1 Hz, 3H), 1.54 (s, 3H), 1.46 (d, *J* = 7.2 Hz, 3H), 1.43 (s, 3H); ^{13}C{^{1}H} NMR ($CDCl_3$, 125 MHz) δ 173.2, 172.7, 170.7, 164.1, 155.5, 136.0, 133.8, 128.62 (2C), 128.57 (2C), 128.5 (2C), 67.3, 63.4, 57.0, 52.2 (2C), 48.6, 29.0, 26.7, 26.0, 24.4, 17.6, 13.4; IR (film) υ_{max} 3274, 2925, 1625, 1536, 1270, 1076 cm^{-1}; HRMS (ESI-TOF) *m*/*z*: $[M + H]^+$ Calcd for $C_{25}H_{34}N_4O_7H$ 503.2506; Found 503.2512.

Summary of NOE distance-restrained calculations.

Manual NMR structural calculations were performed to generate conformational ensembles of all the peptides that were studied. The ensembles were generated using the simulated annealing algorithm CYANA[35] in conjunction with ROESY chemical shift and peak data for the peptides **1**, **2a–c**, and **3a–c**. Dihedral restraints were not used due to the presence of multiple nonstandard amino acids, which lack sufficient secondary chemical shift analysis data. The final structural ensemble for each peptide consists of the 10 lowest-energy conformations as determined by the CYANA objective-function from 100 preliminary structures.

Procedure for proteolysis assays of 1, 2a–c, and 3a–c.

Pronase E from *Streptomyces griseus* (EC 232–909-5) was purchased from Sigma-Aldrich. This mixture of enzymes was dissolved in 1X PBS buffer (10 mM sodium phosphate, 137

mM NaCl, 2.7 mM KCl buffer, pH 7.4) at a concentration of 0.881 mg/mL. Then, solutions of each peptide (**1**, **2a**, **2b**, **2c**, **3a**, **3b**, and **3c**) in 1X PBS buffer (0.50 mM, 0.5 mL) at 38 °C were treated with an aliquot (200 μL) of the Pronase E solution. Aliquots (50 μL) were removed after 0, 15, 30, 45, 60, 90, and 120 min. The aliquots were quenched with glacial acetic acid (20 μL), diluted to 75 μL with 1X PBS buffer, and analyzed by HPLC (Phenomenex Jupiter C18, 5 μm particle size, 300 Å pore size, 4.6 ´ 250 mm, 75 μL injection volume, 40%– 90% CH_3CN in H_2O gradient over 30 min, then 95% CH_3CN in H_2O for 10 min, flow rate: 1 mL/min).

General procedure for thiol reactivity assays.

A solution of ΔAA-containing peptide **2** or **3** (typically 0.010–0.015 mmol) in DMSO-d_6 (600 μL) containing a small amount (<1 mg) of 1,3,5-trimethoxybenzene as an internal standard was treated with 2 equiv of a freshly prepared 0.5 M solution of cysteamine in DMSO-d_6 (typically 40–60 μL). ^{1}H NMR spectra were acquired at various times, and disappearance of the starting peptide was quantified by comparing the integration values of diagnostic signals to the signals of the internal standard. In cases where the peptide was unreactive at room temperature, the solution was heated at successively higher temperatures (60 °C, 80 °C, and 100 °C) and ^{1}H NMR spectra were acquired intermittently. As cysteamine degraded slowly, experiments were halted once it was completely absent from the solution according to ^{1}H NMR.

Supplementary Material

Refer to Web version on PubMed Central for supplementary material.

Acknowledgment.

We thank the National Institutes of Health (1R15GM114789-01A1 and 3R15GM114789-01A1S1) and Brigham Young University (Undergraduate Research Awards to M.A.L. and D.W.K.) for support. Funding for S.T.M. and G.D. was provided by the National Science Foundation Chemistry and Biochemistry REU Site to Prepare Students for Graduate School and an Industrial Career under award CHE-1757627.

REFERENCES

(1). (a)Henninot A; Collins JC; Nuss JM The Current State of Peptide Drug Discovery: Back to the Future? J. Med. Chem 2018, 61, 1382–1414. [PubMed: 28737935] (b)Tsomaia N Peptide Therapeutics: Targeting the Undruggable Space. Eur. J. Med. Chem 2015, 94, 459–470. [PubMed: 25591543] (c)Fosgerau K; Hoffmann T Peptide Therapeutics: Current Status and Future Directions. Drug Discovery Today 2015, 20, 122–128. [PubMed: 25450771] (d)Kaspar AA; Reichert JM Future Directions for Peptide Therapeutics Development. Drug Discovery Today 2013, 18, 807–817. [PubMed: 23726889] (e)Craik DJ; Fairlie DP; Liras S; Price D The Future of Peptide-Based Drugs. Chem. Biol. Drug Des 2013, 81, 136–147. [PubMed: 23253135]

(2). (a)Webster AM; Cobb SL Recent Advances in the Synthesis of Peptoid Macrocycles. Chem. - Eur. J 2018, 24, 7560–7573. [PubMed: 29356125] (b)Sun J; Zuckermann RN Peptoid Polymers: A Highly Designable Bioinspired Material. ACS Nano 2013, 7, 4715–4732. [PubMed: 23721608] (c)Yoo B; Shin SBY; Huang ML; Kirshenbaum K Peptoid Macrocycles: Making the Rounds with Peptidomimetic Oligomers. Chem. - Eur. J 2010, 16, 5528–5537. [PubMed: 20414912] (d)Fowler SA; Blackwell HE Structure–Function Relationships in Peptoids: Recent Advances Toward Deciphering the Structural Requirements for Biological Function. Org. Biomol. Chem 2009, 7, 1508–1524. [PubMed: 19343235]

(3). (a)Cabrele C; Martinek TA; Reiser O; Berlicki Ł Peptides Containing β-Amino Acid Patterns: Challenges and Successes in Medicinal Chemistry. J. Med. Chem 2014, 57, 9718–9739. [PubMed: 25207470] (b)Horne WS; Gellman SH Foldamers with Heterogeneous Backbones. Acc. Chem. Res 2008, 41, 1399–1408. [PubMed: 18590282] (c)Seebach D; Gardiner J β-Peptidic Peptidomimetics. Acc. Chem. Res 2008, 41, 1366–1375. [PubMed: 18578513] (d)Cheng RP; Gellman SH; DeGrado WF β-Peptides: From Structure to Function. Chem. Rev 2001, 101, 3219–3252. [PubMed: 11710070]

(4). (a)Reguera L; Rivera DG Multicomponent Reaction Toolbox for Peptide Macrocyclization and Stapling. Chem. Rev 2019, 119, 9836–9860. [PubMed: 30990310] (b)Lau YH; de Andrade P; Wu Y; Spring DR Peptide Stapling Techniques Based on Different Macrocyclisation Chemistries. Chem. Soc. Rev 2015, 44, 91–102. [PubMed: 25199043] (c)Cromm PM; Spiegel J; Grossmann TN Hydrocarbon Stapled Peptides as Modulators of Biological Function. ACS Chem. Biol 2015, 10, 1362–1375. [PubMed: 25798993] (d)Walensky LD; Bird GH Hydrocarbon-Stapled Peptides: Principles, Practice, and Progress. J. Med. Chem 2014, 57, 6275–6288. [PubMed: 24601557]

5. Patgiri A; Jochim AL; Arora PS A Hydrogen Bond Surrogate Approach for Stabilization of Short Peptide Sequences in α-Helical Conformation. Acc. Chem. Res 2008, 41, 1289–1300. [PubMed: 18630933]

(6). (a)Teng P; Shi Y; Sang P; Cai J γ-AAPeptides as a New Class of Peptidomimetics. Chem. - Eur. J 2016, 22, 5458–5466. [PubMed: 26945679] (b)Shi Y; Teng P; Sang P; She F; Wei L; Cai J γ-AAPeptides: Design, Structure, and Applications. Acc. Chem. Res 2016, 49, 428–441. [PubMed: 26900964]

7. Weinstock MT; Francis JN; Redman JS; Kay MS Protease-Resistant Peptide Design—Empowering Nature's Fragile Warriors Against HIV. Biopolymers (Pept. Sci.) 2012, 98, 431–442.

8. Toniolo C; Formaggio F; Kaptein B; Broxterman QB You Are Sitting on a Gold Mine! Synlett 2006, 1295–1310.

9. Sarnowski MP; Kang CW; Elbatrawi YM; Wojtas L; Del Valle JR Peptide N-Amination Supports β-Sheet Conformations. Angew. Chem., Int. Ed 2017, 56, 2083–2086.

(10). (a)Lubell WD; Khashper A Design, Synthesis, Conformational Analysis and Application of Indolizidin-2-one Dipeptide Mimics. Org. Biomol. Chem 2014, 12, 5052–5070. [PubMed: 24899358] (b)MacDonald M; Aubé J Approaches to Cyclic Peptide β-Turn Mimics. Curr. Org. Chem 2001, 5, 417–438.

(11). (a)Nischan N; Hackenberger CPR Site-specific PEGylation of Proteins: Recent Developments. J. Org. Chem 2014, 79, 10727–10733. [PubMed: 25333794] (b)Jevševar S; Kunstelj M; Porekar VG PEGylation of Therapeutic Proteins. Biotechnol J 2010, 5, 113–128. [PubMed: 20069580] (c)Harris JM; Chess RB Effect of PEGylation on Pharmaceuticals. Nat. Rev. Drug Discovery 2003, 2, 214–221. [PubMed: 12612647]

(12). (a)Liu Z; Chen X Simple Bioconjugate Chemistry Serves Great Clinical Advances: Albumin as a Versatile Platform for Diagnosis and Precision Therapy. Chem. Soc. Rev 2016, 45, 1432–1456. [PubMed: 26771036] (b)Elsadek B; Kratz F Impact of Albumin on Drug Delivery – New Applications on the Horizon. J. Controlled Release 2012, 157, 4–28.(c)Pollaro L; Heinis C Strategies to Prolong the Plasma Residence Time of Peptide Drugs. Med. Chem. Commun 2010, 1, 319–324.

13. O'Banion CP; Nguyen LT; Wang Q; Priestman MA; Holly SP; Parise LV; Lawrence DS The Plasma Membrane as a Reservoir, Protective Shield, and Light-Triggered Launch Pad for Peptide Therapeutics. Angew. Chem., Int. Ed 2016, 55, 950–954.

14. https://www.fda.gov/drugs/development-approval-process-drugs/new-drugs-fda-cders-new-molecular-entities-and-new-therapeutic-biological-products

(15). (a)English ML; Stammer CH The Enzyme Stability of Dehydropeptides. Biochem. Biophys. Res. Commun 1978, 83, 1464–1467. [PubMed: 697874] (b)English ML; Stammer CH D-Ala^{2}, Δ^{Z}Phe^{4}-Methionine Enkephalin Amide, a Dehydropeptide Hormone. Biochem. Biophys. Res. Commun 1978, 85, 780–782. [PubMed: 216357] (c)Shimohigashi Y; Chen H-C; Stammer CH The Enzyme Stability of Dehydro-Enkephalins. Peptides 1982, 3, 985–987. [PubMed: 7167404] (d)Shimohigashi Y; Stammer CH Dehydro-enkephalins. Part 7. A Potent Dehydroleucine-enkephalin Resistant to Carboxypeptidase. J. Chem. Soc., Perkin Trans 1 1983, 803–808.

(16). (a)Daniel RM; Cowan DA; Morgan HW; Curran MP A Correlation Between Protein Thermostability and Resistance to Proteolysis. Biochem. J 1982, 207, 641–644. [PubMed: 6819862] (b)Imoto T; Yamada H; Ueda T Unfolding Rates of Globular Proteins Determined by Kinetics of Proteolysis. J. Mol. Biol 1986, 190, 647–649. [PubMed: 3783715] (c)Parsell DA; Sauer RT The Structural Stability of a Protein Is an Important Determinant of Its Proteolytic Susceptibility in *Escherichia coli*. J. Biol. Chem 1989, 264, 7590–7595. [PubMed: 2651442] (d)Klink TA; Raines RT Conformational Stability Is a Determinant of Ribonuclease A Cytotoxicity. J. Biol. Chem 2000, 275, 17463–17467. [PubMed: 10747991] (e)Ahmad S; Kumar V; Ramanand KB; Rao NM Probing Protein Stability and Proteolytic Resistance by Loop Scanning: A Comprehensive Mutational Analysis. Protein Sci 2012, 21, 433–446. [PubMed: 22246996]

(17). (a)Rajashankar KR; Ramakumar S; Chauhan VS Design of a Helical Motif Using α,β-Dehydrophenylalanine Residues: Crystal Structure of Boc-Val-ΔPhe-Phe-Ala-Phe-ΔPhe-Val-ΔPHe-Gly-OCH_3, a 3_{10}-Helical Nonapeptide. J. Am. Chem. Soc 1992, 114, 9225–9226. (b)Bhandary KK; Chauhan VS Peptide Design 3_{10}-Helical Conformation of a Linear Pentapeptide Containing Two Dehydrophenylalanines, Boc-Gly-Δ^Z-Phe-Leu-Δ^ZPhe-Ala-$NHCH_3$. Biopolymers 1993, 33, 209–217. [PubMed: 8485295] (c)Pieroni O; Fissi A; Jain RM; Chauhan VS Solution Structure of Dehydropeptides: A CD Investigation. Biopolymers 1996, 38, 97–108. [PubMed: 8679945] (d)Jain RM; Rajashankar KR; Ramakumar S; Chauhan VS First Observation of Left-Handed Helical Conformation in a Dehydro Peptide Containing Two L-Val Residues. Crystal and Solution Structure of Boc-L-Val-ΔPhe-ΔPhe-ΔPhe-L-Val-OMe. J. Am. Chem. Soc 1997, 119, 3205–3211.

(18). (a)Jain R; Chauhan VS Conformational Characteristics of Peptides Containing α,β-Dehydroamino Acid Residues. Biopolymers (Pept. Sci.) 1996, 40, 105–119.(b)Mathur P; Ramakumar S; Chauhan VS Peptide Design Using α,β-Dehydroamino Acids: From β-Turns to Helical Hairpins. Biopolymers (Pept. Sci.) 2004, 76, 150–161.(c)Gupta M; Chauhan VS De Novo Design of α,β-Didehydrophenylalanine Containing Peptides: From Models to Applications. Biopolymers 2011, 95, 161–173. [PubMed: 21053260]

(19). (a)Singh TP; Narula P; Patel HC α,β-Dehydro Residues in the Design of Peptide and Protein Structures. Acta Crystallogr 1990, B46, 539–545.(b)Zecchini GP; Paradisi MP; Torrini I; Lucente G; Gavuzzo E; Mazza F; Pochetti G; Paci M; Sette M; Di Nola A; Veglia G; Traniello S; Spisani S Synthesis, Conformation, and Activity of HCO-Met-Δ^ZLeu-Phe-Ome, an Active Analogue of Chemotactic *N*-Formyltripeptides. Biopolymers 1993, 33, 437–451. [PubMed: 8461452] (c)Inai Y; Oshikawa T; Yamashita M; Hirabayashi T; Hirako T Structural and Conformational Properties of (Z)-β-(1-Naphthyl)-dehydroalanine Residue. Biopolymers 2001, 58, 9–19. [PubMed: 11072225] (d)Inai Y; Hirabayashi T A Helical Arrangement of β-Substituents of Dehydropeptides: Synthesis and Conformational Study of Sequential Nona- and Dodecapeptides Possessing (Z)-β-(1-Naphthyl)-dehydroalanine Residues. Biopolymers 2001, 59, 356–369. [PubMed: 11514939] (e)Buczek A; Siodłak D; Bujak M; Broda MA Effects of Side-Chain Orientation on the Backbone Conformation of the Dehydrophenylalanine Residue. Theoretical and X-ray Study. J. Phys. Chem. B 2011, 115, 4295–4306. [PubMed: 21443240] (f)Jewginski M; Latajka R; Krezel A; Haremza K; Makowski M; Kafarski P Influence of Solvents on Conformation of Dehydropeptides. J. Mol. Struct 2013, 1035, 129–139.(g)Buczek A; Makowski M; Jewgiński M; Latajka R; Kupka T; Broda MA Toward Engineering Efficient Peptidomimetics. Screening Conformational Landscape of Two Modified Dehydroaminoacids. Biopolymers 2014, 101, 28–40. [PubMed: 23606332]

20. Le DN; Riedel J; Kozlyuk N; Martin RW; Dong VM Cyclizing Pentapeptides: Mechanism and Application of Dehydrophenylalanine as a Traceless Turn-Inducer. Org. Lett 2017, 19, 114–117. [PubMed: 27973857]

(21). (a)Yamada K; Shinoda S.-s.; Oku H; Komagoe K; Katsu T; Katakai R Synthesis of Low-Hemolytic Antimicrobial Dehydropeptides Based on Gramicidin S. J. Med. Chem 2006, 49, 7592–7595. [PubMed: 17181140] (b)Yamada K; Kodaira M; Shinoda S.-s.; Komagoe K; Oku H; Katakai R; Katsu T; Matsuo I Structure–Activity Relationships of Gramicidin S Analogs Containing (β−3-Pyridyl)-α,β-dehydroalanine Residues on Membrane Permeability. Med. Chem. Commun 2011, 2, 644–649.(c)Grigoryan HA; Hambardzumyan AA; Mkrtchyan MV; Topuzyan VO; Halebyan GP; Asatryan RS α,β-Dehydrophenylalanine Choline Esters, a New Class of

Reversible Inhibitors of Human Acetylcholinesterase and Butyrylcholinesterase. Chem.-Biol. Interact 2008, 171, 108–116. [PubMed: 17980356] (d)Pathak S; Chauhan VS Rationale-Based, *De Novo* Design of Dehydrophenylalanine-Containing Antibiotic Peptides and Systematic Modification in Sequence for Enhanced Potency. Antimicrob. Agents Chemother 2011, 55, 2178–2188. [PubMed: 21321136] (e)Mishra A; Misra A; Vaishnavi TS; Thota C; Gupta M; Ramakumar S; Chauhan VS Conformationally Restricted Short Peptides Inhibit Human Islet Amyloid Polypeptide (hIAPP) Fibrillization. Chem. Commun 2013, 49, 2688–2690.(f)Giordano C; Punzi P; Lori C; Chiaraluce R; Consalvi V β-Sheet Breaker Peptides Containing α,β-Dehydrophenylalanine: Synthesis and In Vitro Activity Studies. ChemPlusChem 2014, 79, 1036–1043.

(22). (a)Yokokawa F; Shioiri T Novel Stereospecific Dehydration of β-Hydroxy-α-amino Acids Using Martin's Sulfurane. Tetrahedron Lett 2002, 43, 8679–8682.(b)Sai H; Ogiku T; Ohmizu H Stereoselective Syntheses of (*E*)-α,β-Dehydroamino Acids and (*E*)-α,β-Dehydropeptides by Stereospecific Dehydration with 1-Ethyl-3-(3-dimethylaminopropyl)carbodiimide (EDC). Synthesis 2003, 201–204.

(23). (a)Yamashita T; Kuranaga T; Inoue M Solid-Phase Total Synthesis of Bogorol A: Stereocontrolled Construction of Thermodynamically Unfavored (*E*)-2-Amino-2-butenamide. Org. Lett 2015, 17, 2170–2173. [PubMed: 25866994] (b)Butler E; Florentino L; Cornut D; Gomez-Campillos G; Liu H; Regan AC; Thomas EJ Synthesis of Macrocyclic Precursors of the Vioprolides. Org. Biomol. Chem 2018, 16, 6935–6960. [PubMed: 30226509]

24. Ueoka R; Ise Y; Ohtsuka S; Okada S; Yamori T; Matsunaga S Yaku'amides A and B, Cytotoxic Linear Peptides Rich in Dehydroamino Acids from the Marine Sponge *Ceratopsion sp*. J. Am. Chem. Soc 2010, 132, 17692–17694. [PubMed: 21121605]

25. Culvenor CCJ; Edgar JA; Mackay MF; Gorst-Allman CP; Marasas WFO; Steyn PS; Vleggaar R; Wessels PL Structure Elucidation and Absolute Configuration of Phomopsin A, a Hexapeptide Mycotoxin Produced by *Phomopsis Leptostromiformis*. Tetrahedron 1989, 45, 2351–2372.

(26). (a)Irschik H, Gerth K, Kemmer T, Steinmetz H, Reichenbach H The Myxovalargins, New Peptide Antibiotics from *Myxococcus Fulvus* (Myxobacterales). I. Cultivation, Isolation and Some Chemical and Biological Properties. J. Antibiot 1983, 36, 6–12. [PubMed: 6432761] (b)Irschik H, Reichenbach H The Mechanism of Action of Myxovalargin A, a Peptide Antibiotic from *Myxococcus Fulvus*. J. Antibiot 1985, 38, 1237–1245. [PubMed: 2415501] (c)Steinmetz H; Irschik H; Reichenbach H; Höfle G Structure Elucidation of the Peptide Antibiotics Myxovalargin A–D. Chem. Pept. Proteins 1989, 4, 13–18.

(27). (a)Pietrzyński G; Rzeszotarska B; Kubica Z Conformational Investigation of α,β-Dehydropeptides. Part IV. β-Turn in Saturated and α,β-Unsaturated Peptides Ac-Pro-Xaa-$NHCH_3$: NMR and IR Studies. Int. J. Peptide Protein Res 1992, 40, 524–531. [PubMed: 1286936] (b)Vijayaraghavan R; Kumar P; Dey S; Singh TP Design of Peptides with α,β-Dehydro Residues: A Dipeptide with a Branched β-Carbon Dehydro Residue at the (*i*+1) Position, Methyl *N*-(Benzyloxycarbonyl)-α,β-didehydrovalyl-L-tryptophanate. Acta Crystallogr., Sect. C 2001, 57, 1220–1221. [PubMed: 11600792] (c)Vijayaraghavan R; Kumar P; Dey S; Singh TP Design of Peptides with Branched β-Carbon Dehydro-residues: Syntheses, Crystal Structures and Molecular Conformations of Two Peptides, (I) *N*-Carbobenzoxy-ΔVal-Ala-Leu-OCH_3 and (II) *N*-Carbobenzoxy-ΔIle-Ala-Leu-OCH_3. J. Pept. Res 2003, 62, 63–69. [PubMed: 12823618] (d)Makker J; Dey S; Mukherjee S; Vijayaraghavan R; Kumar P; Singh TP Design of Peptides with α,β-Dehydro-residues: Synthesis, Crystal Structure and Molecular Conformation of a Tetrapeptide *Z*-ΔVal-Val-ΔPhe-Ile-Ome. J. Mol. Struct 2003, 654, 119–124.(e)Siodłak D; Rzeszotarska B; Broda MA; Kozioł AE; Kołodziejczyk E Conformational Investigation of α,β-Dehydropeptides. *N*-Acetyl-α,β-dehydrovaline-*N*′,*N*′-dimethylamide. Acta Biochim. Pol 2004, 51, 145–152. [PubMed: 15094835] (f)Broda MA; Siodłak D; Rzeszotarska B Conformational Investigation of α,β-Dehydropeptides. XV: *N*-Acetyl-α,β-dehydroamino Acid *N*′*N*′-Dimethylamides: Conformational Properties from Infrared and Thereorectical Studies. J. Pept. Sci 2005, 11, 546–555. [PubMed: 15782429] (g)Siodłak D; Grondys J; Lis T; Bujak M; Broda MA; Rzeszotarska B The Conformational Properties of Dehydrobutyrine and Dehydrovaline: Theoretical and Solid-State Conformational Studies. J. Pept. Sci 2010, 16, 496–505. [PubMed: 20645424] (h)Siodłak D; Bujak M; Staś M Intra- and Intermolecular Forces Dependent Main Chain Conformations of Esters of α,β-Dehydroamino Acids. J. Mol. Struct 2013, 1047, 229–236.

28. For a review on bulky ΔAAs, see:Jiang J; Ma Z; Castle SL Bulky α,β-Dehydroamino Acids: Their Occurrence in Nature, Synthesis, and Applications. Tetrahedron 2015, 71, 5431–5451.
29. Jiang J; Luo S; Castle SL Solid-Phase Synthesis of Peptides Containing Bulky Dehydroamino Acids. Tetrahedron Lett 2015, 56, 3311–3313.
30. Jalan A; Kastner DW; Webber KGI; Smith MS; Price JL; Castle SL Bulky Dehydroamino Acids Enhance Proteolytic Stability and Folding in β-Hairpin Peptides. Org. Lett 2017, 19, 5190–5193. [PubMed: 28910115]
31. Nagaraj R; Shamala N; Balaram P Stereochemically Constrained Linear Peptides. Conformations of Peptides Containing α-Aminoisobutyric Acid. J. Am. Chem. Soc 1979, 101, 16–20.
32. Ma Z; Naylor BC; Loertscher BM; Hafen DD; Li JM; Castle SL Regioselective Base-Free Intermolecular Aminohydroxylations of Hindered and Functionalized Alkenes. J. Org. Chem 2012, 77, 1208–1214. [PubMed: 22188212]
33. Ross AC; Liu H; Pattabiraman VR; Vederas JC Synthesis of the Lantibiotic Lactocin S Using Peptide Cyclizations on Solid Phase. J. Am. Chem. Soc 2010, 132, 462–463. [PubMed: 20017553]
34. Wołczański G; Lisowski M A General Method for Preparation of *N*-Boc-Protected or *N*-Fmoc-Protected α,β-Didehydropeptide Building Blocks and Their Use in the Solid-Phase Peptide Synthesis. J. Pept. Sci 2018, 24, e3091. [PubMed: 29862598]
(35). (a)Güntert P; Mumenthaler C; Wüthrich K Torsion Angle Dynamics for NMR Structure Calculation with the New Program DYANA. J. Mol. Biol 1997, 273, 283–298. [PubMed: 9367762] (b)Yilmaz EM; Güntert P NMR Structure Calculation for All Small Molecule Ligands and Non-Standard Residues from the PDB Chemical Component Dictionary. J. Biomol. NMR 2015, 63, 21–37. [PubMed: 26123317]
36. Cline LL; Waters ML The Structure of Well-Folded β-Hairpin Peptides Promotes Resistance to Peptidase Degradation. Biopolymers (Pept. Sci.) 2009, 92, 502–507.
37. Yang B; Wang N; Schnier PD; Zheng F; Zhu H; Polizzi NF; Ittuveetil A; Saikam V; DeGrado WF; Wang Q; Wang PG; Wang L Genetically Introducing Biochemically Reactive Amino Acids Dehydroalanine and Dehydrobutyrine in Proteins. J. Am. Chem. Soc 2019, 141, 7698–7703. [PubMed: 31038942]
38. Chatterjee C; Paul M; Xie L; van der Donk WA Biosynthesis and Mode of Action of Lantibiotics. Chem. Rev 2005, 105, 633–683. [PubMed: 15700960]
(39). (a)Gutiérrez A; Osante I; Cativiela C Synthesis of cis- and trans-(±)-3-Mercaptoproline and Pipecolic Acid Derivatives via thio-Michael Addition. Tetrahedron Lett 2018, 59, 1661–1665. (b)Villadsen NL; Hansen BK; Svenningsen EB; Jørgensen KH; Tørring T; Poulsen TB Stendomycin and Pantomycin Are Identical Natural Products: Preparation of a Functionalized Bioactive Analogue. J. Org. Chem 2018, 83, 7303–7308. [PubMed: 29724097]
40. Aydillo C; Avenoza A; Busto JH; Jiménez-Osés G; Peregrina JM; Zurbano MM A Biomimetic Approach to Lanthionines. Org. Lett 2012, 14, 334–337. [PubMed: 22176606]
41. Avonto C; Taglialatela-Scafati O; Pollastro F; Minassi A; Di Marzo V; De Petrocellis L; Appendino G An NMR Spectroscopic Method to Identify and Classify Thio-Trapping Agents: Revival of Michael Acceptors for Drug Discovery? Angew. Chem., Int. Ed 2011, 50, 467–471.
42. A preliminary version of this manuscript was deposited on the ChemRxiv preprint server:Joaquin D; Lee MA; Kastner DW; Singh J; Morrill ST; Damstedt G; Castle SL Impact of Dehydroamino Acids on the Structure and Stability of Incipient 3_{10}-Helical Peptides. ChemRxiv 2019, 10.26434/chemrxiv.9968375.v1.

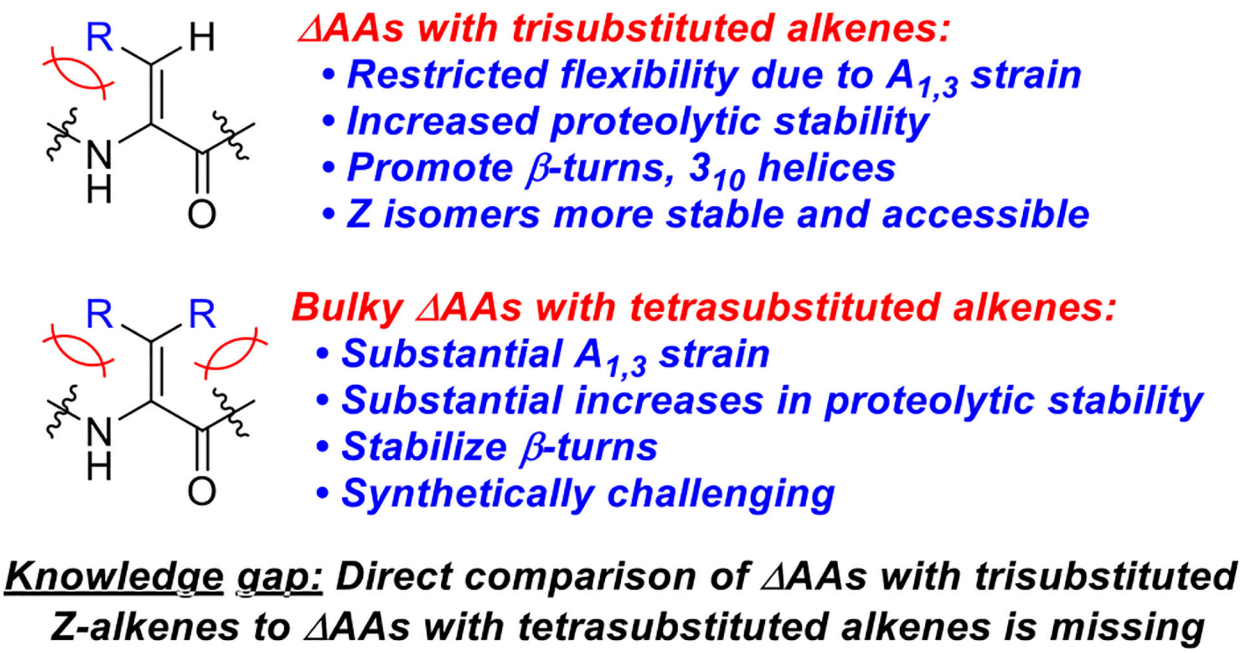

Figure 1.
Two types of dehydroamino acids.

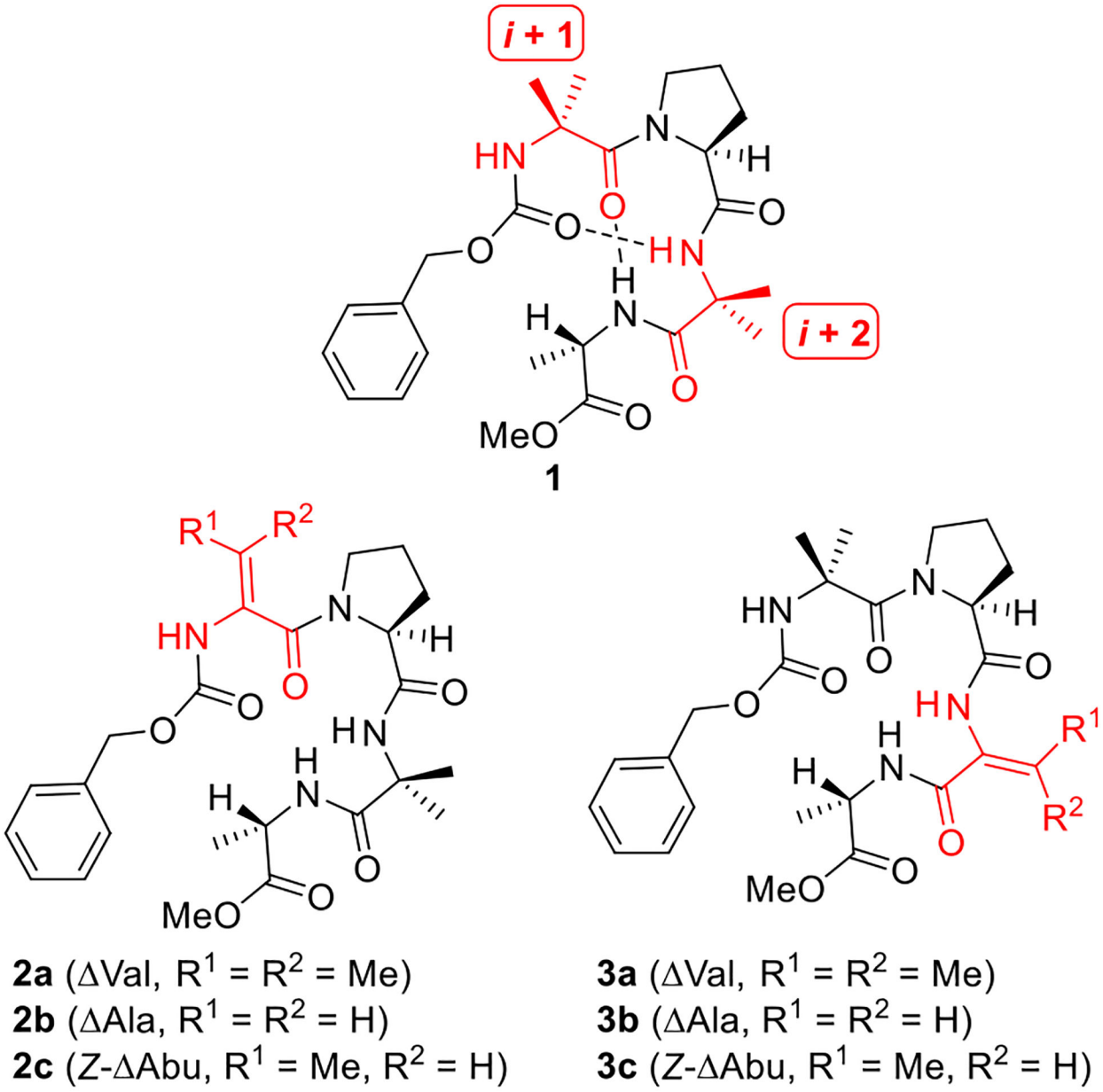

Figure 2.
Balaram's incipient 3_{10} helical peptide (**1**) and proposed ΔAA-containing variants (**2** and **3**).

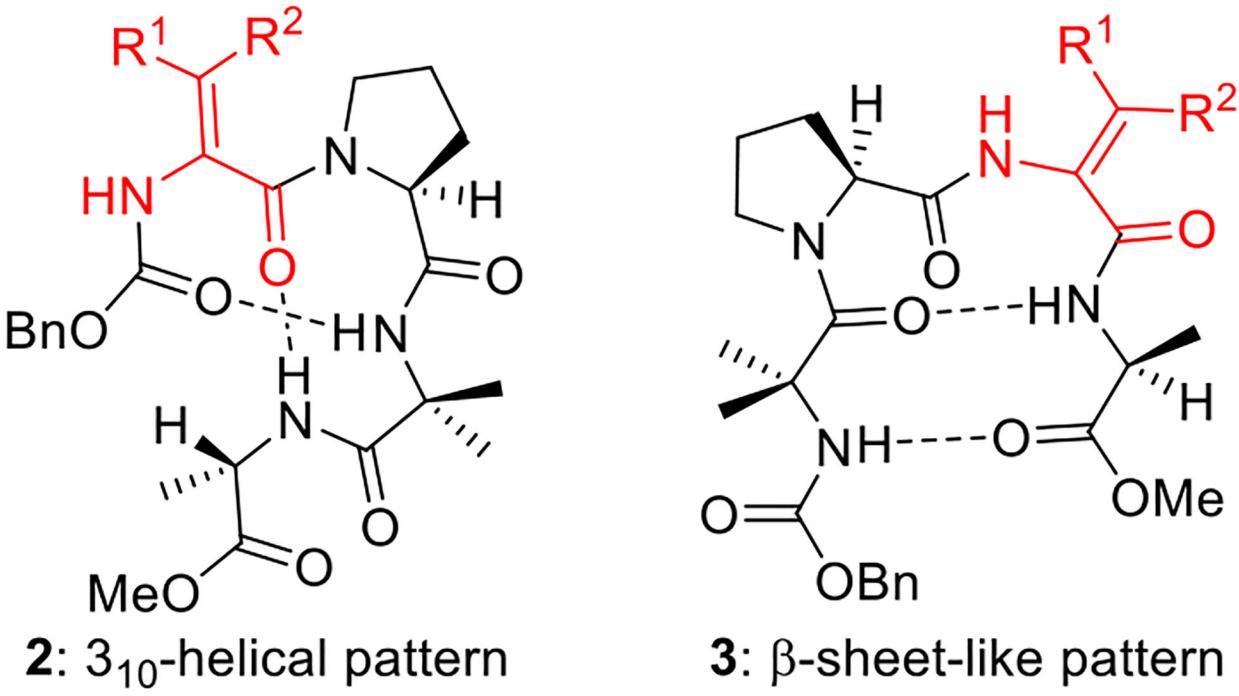

Figure 3.
3_{10}-Helical and β-sheet-like conformations.

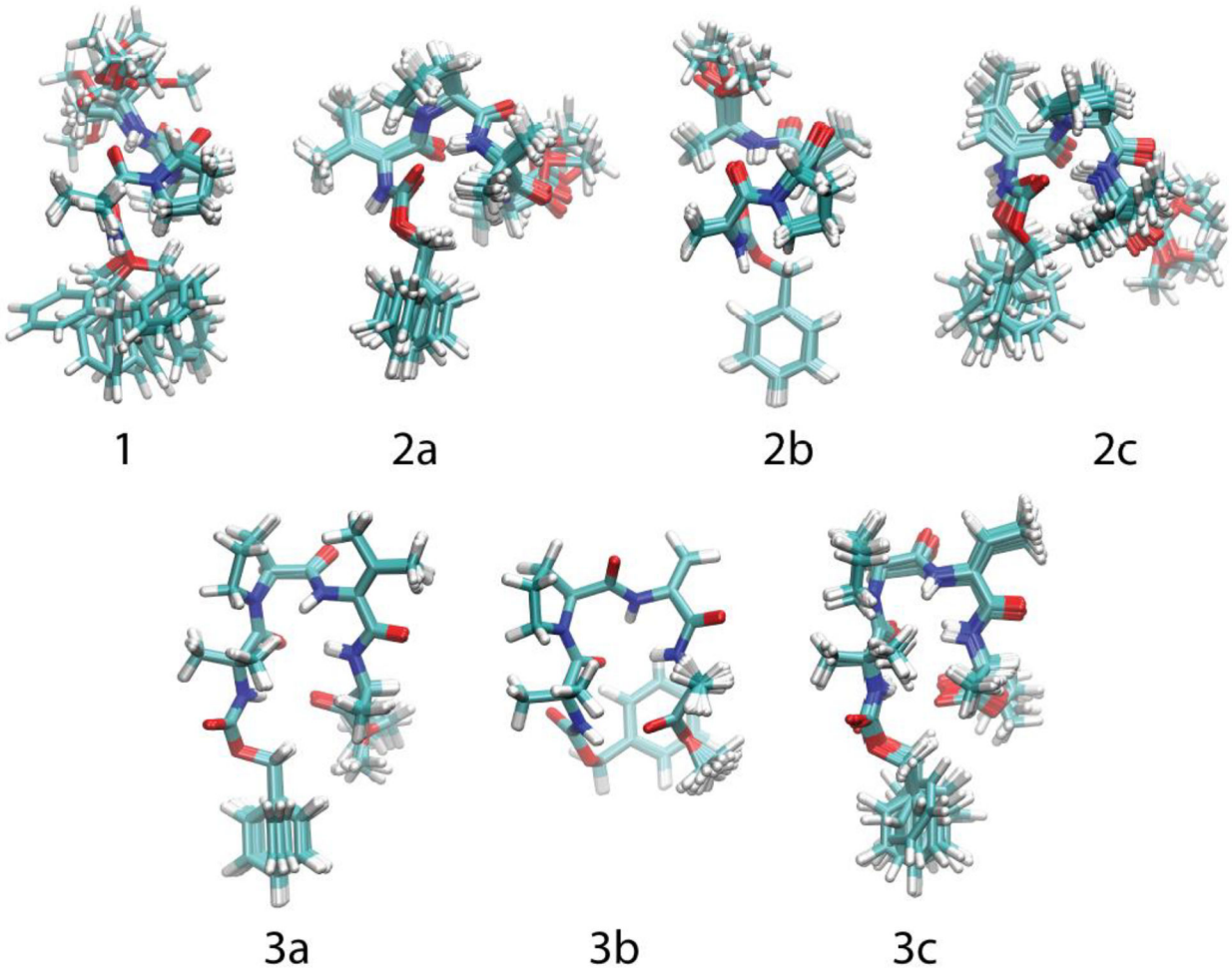

Figure 4.
Solution-phase structures of **1**, **2a–c**, and **3a–c** as calculated using NOE distance restraints.

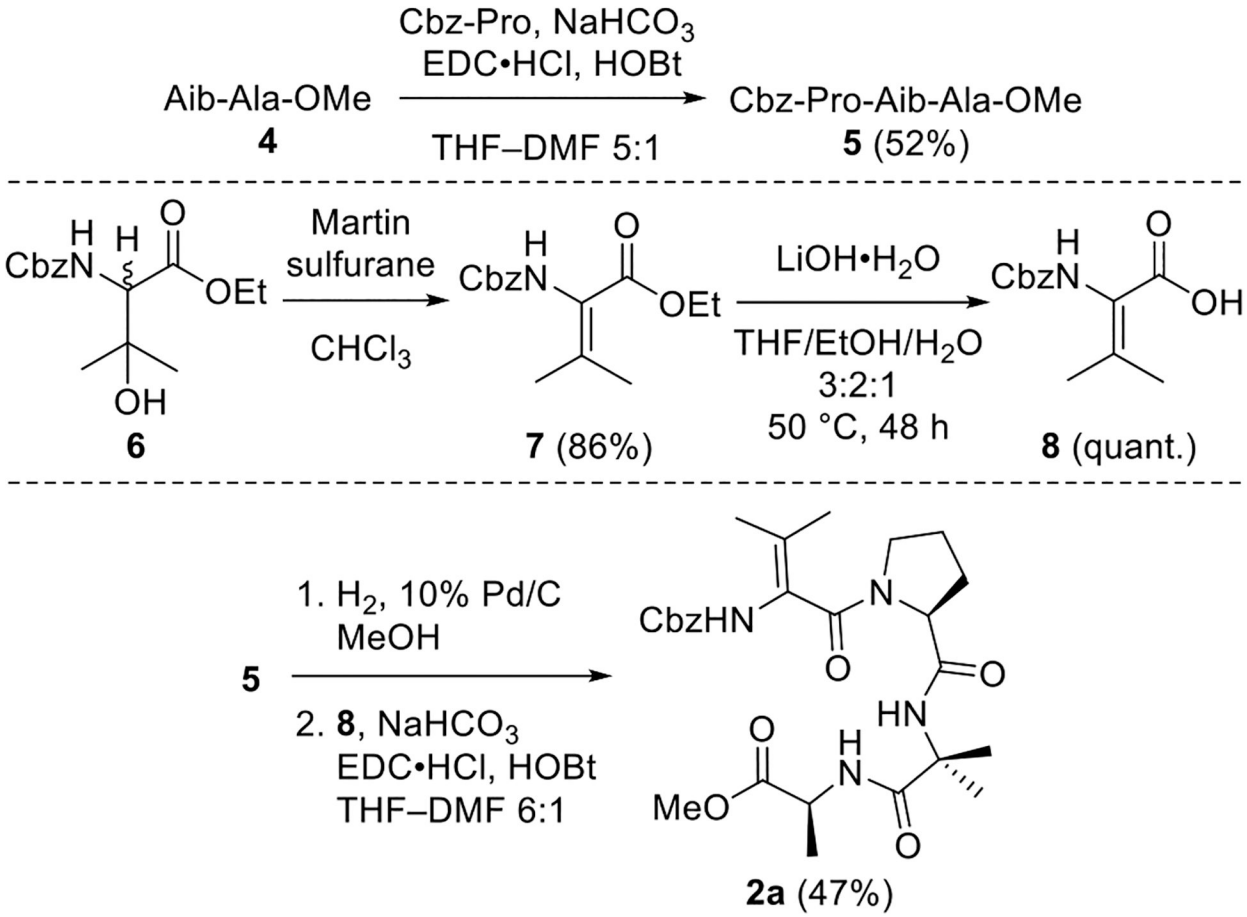

Scheme 1. Synthesis of ΔVal Analog 2a

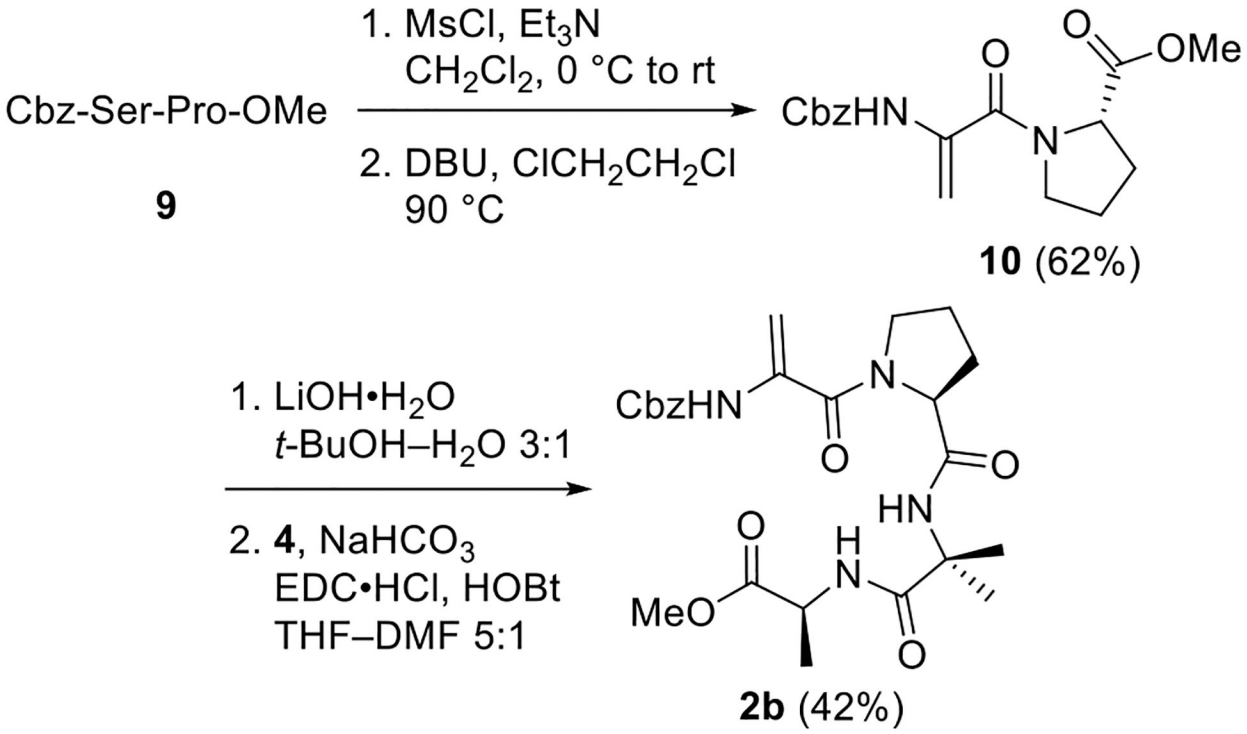

Scheme 2. Synthesis of ΔAla Analog 2b

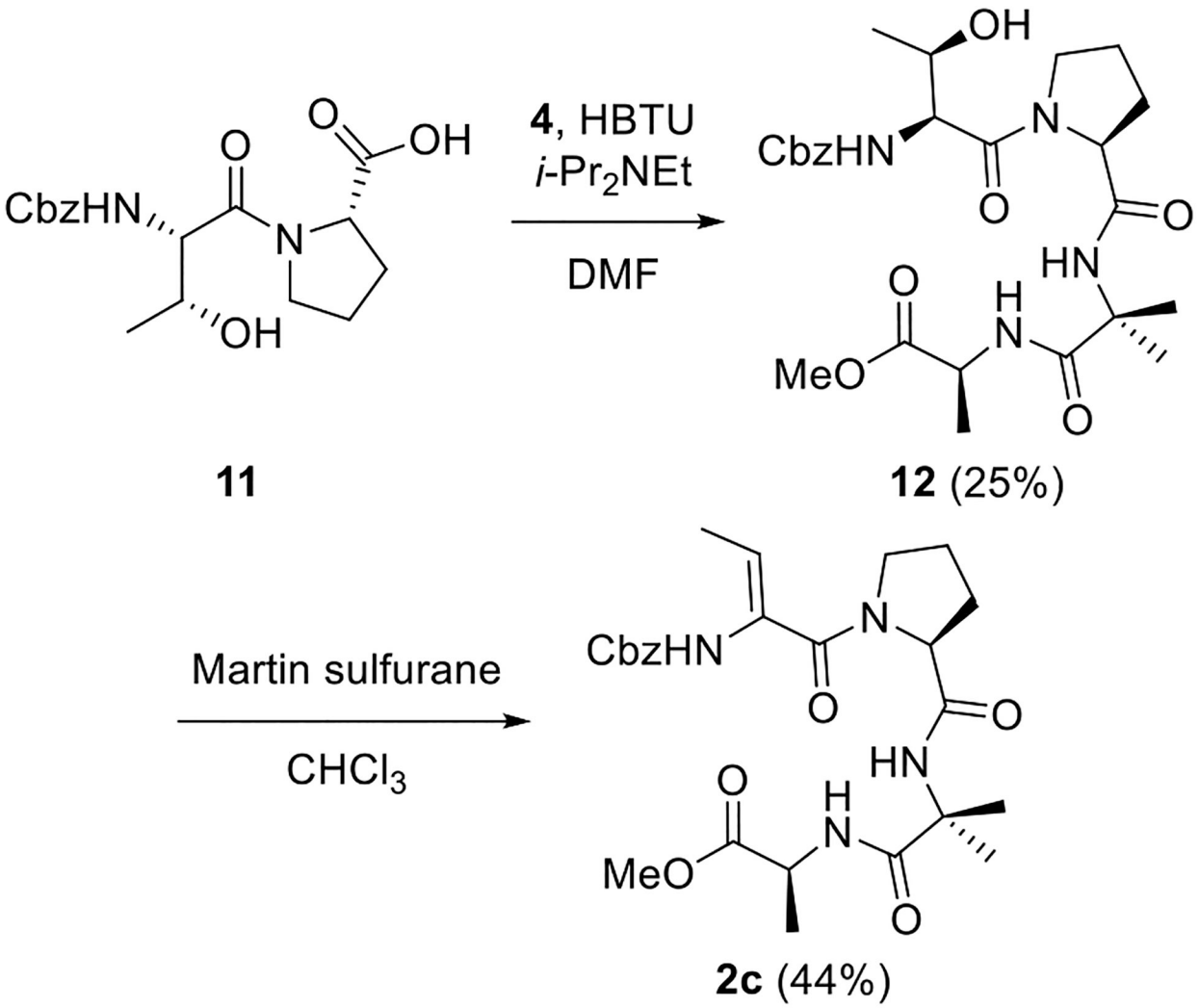

Scheme 3. Synthesis of *Z*-ΔAbu Analog 2c

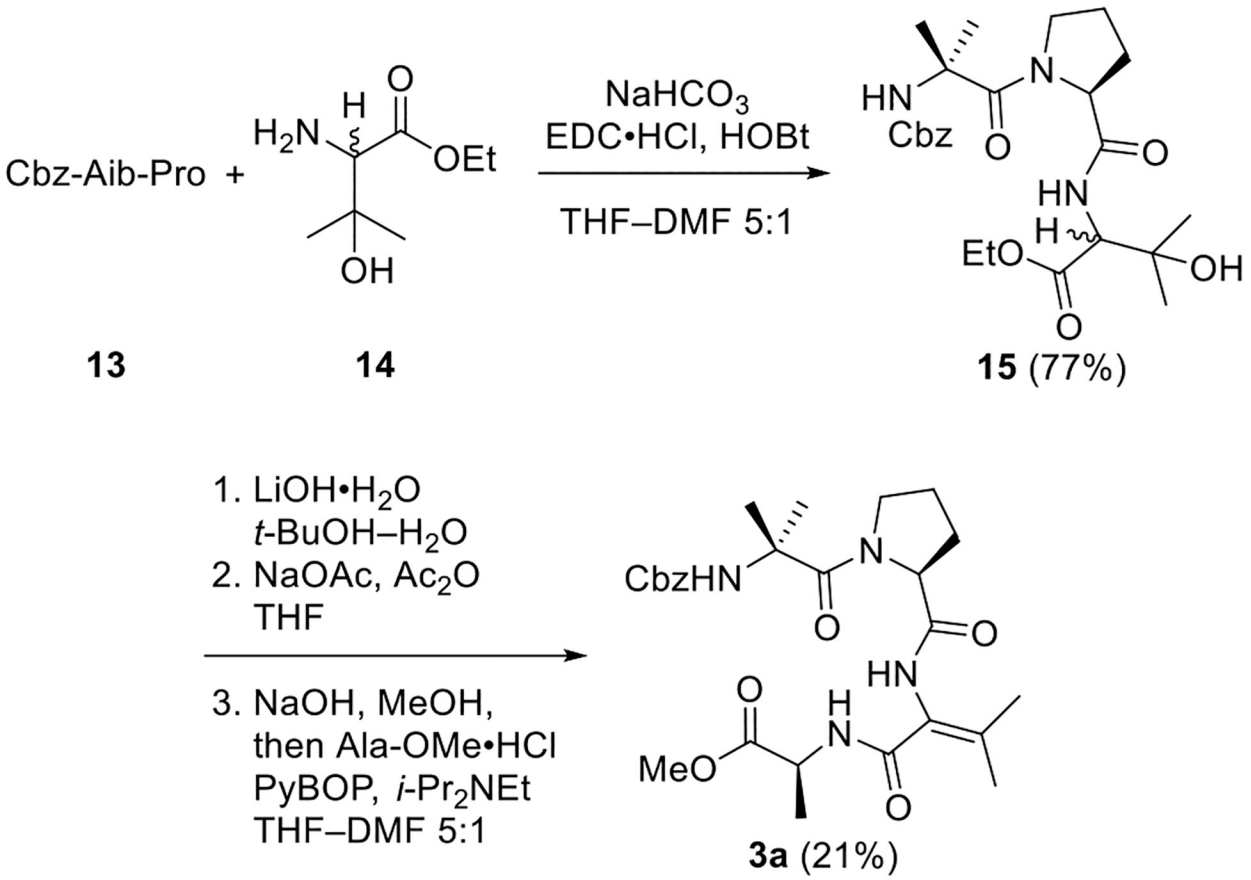

13 14 **15** (77%)

3a (21%)

Scheme 4. Synthesis of ΔVal Analog 3a

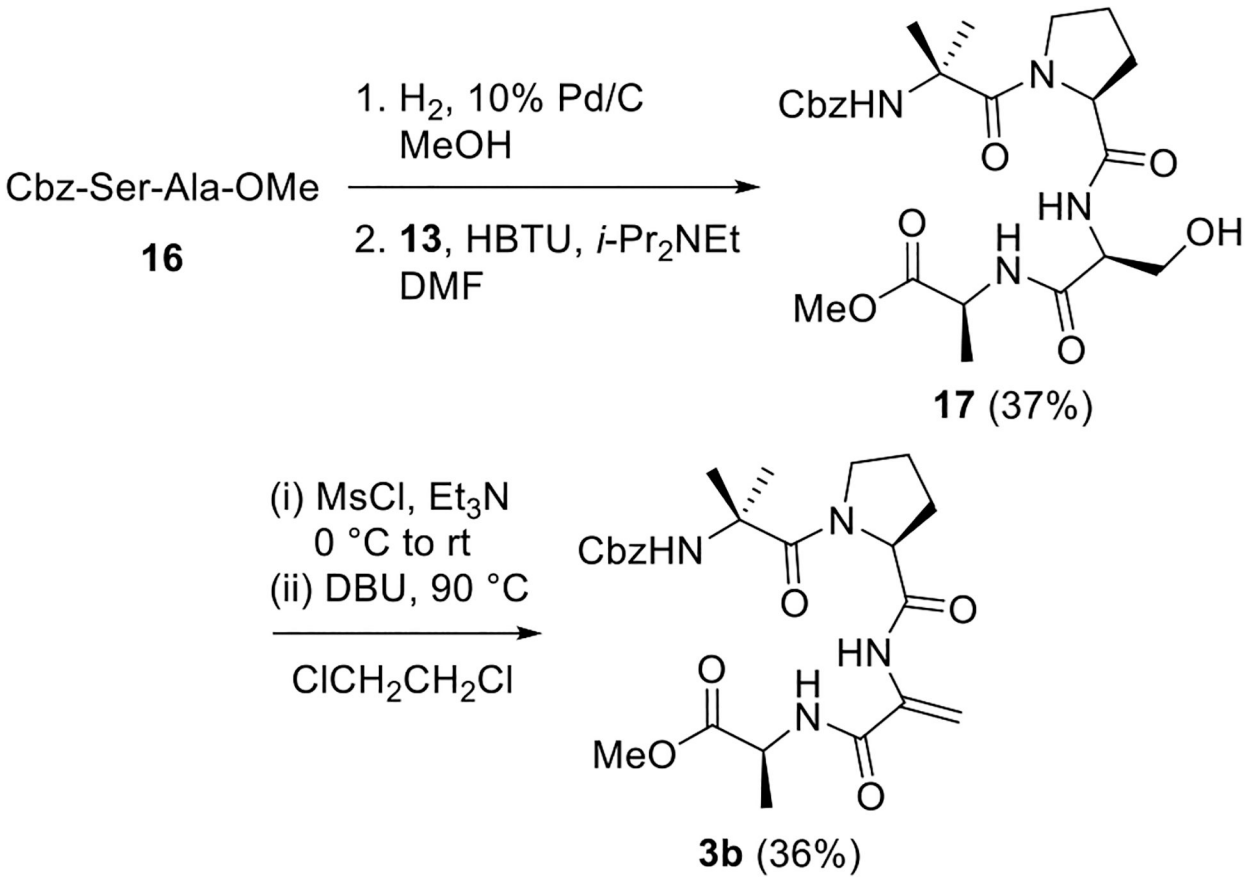

Scheme 5. Synthesis of ΔAla Analog 3b

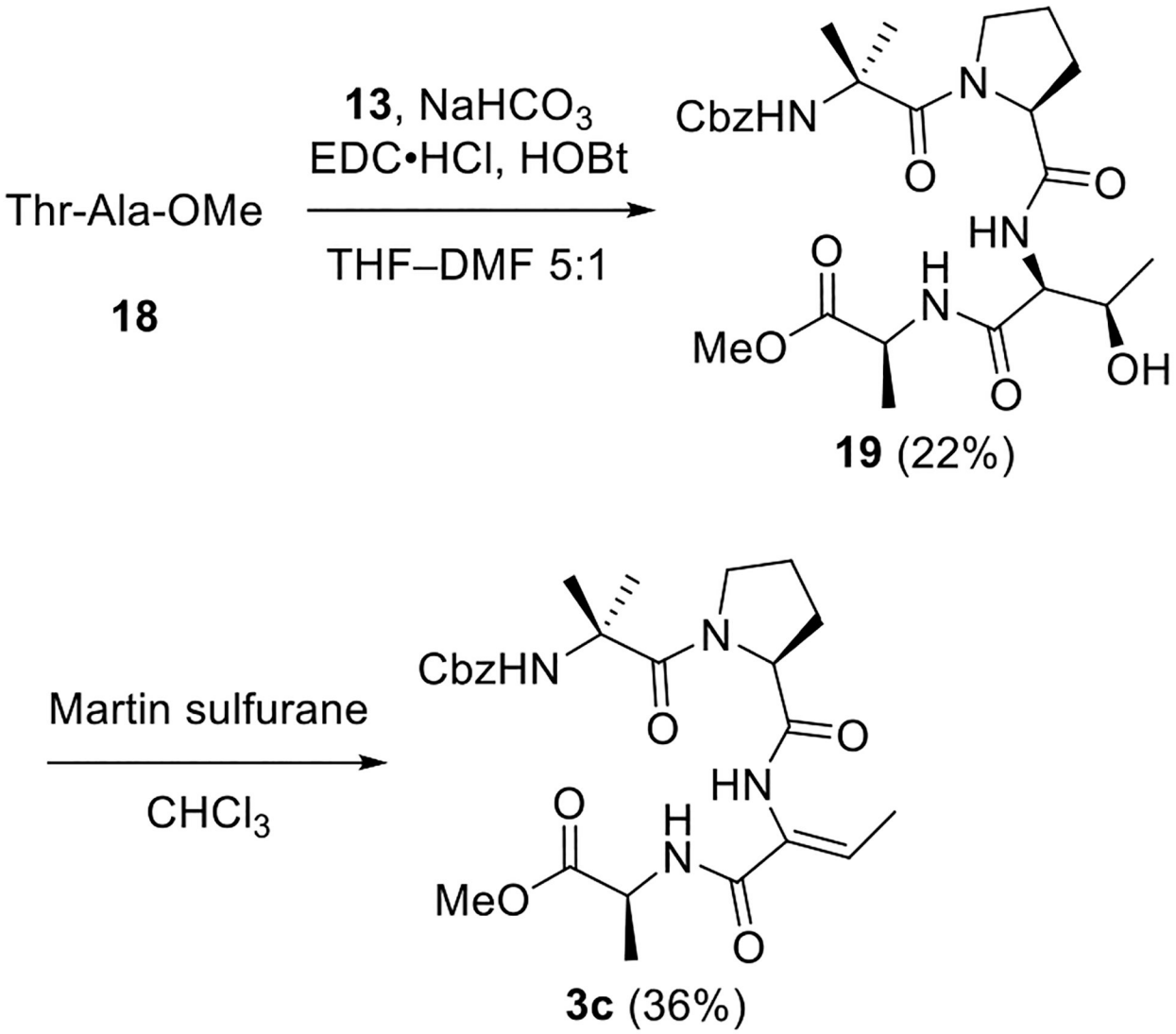

Scheme 6. Synthesis of *Z*-ΔAbu Analog 3c

Table 1.

Proteolysis of 1 and Analogs by Pronase[a]

peptide	amount remaining after 30 min (%)
1	31
2a	31
2b	9
2c	21
3a	61
3b	3
3c	58

[a]Solutions of peptides (0.5 mM, 500 μL) in 1X PBS buffer (10 mM sodium phosphate, 137 mM NaCl, 2.7 mM KCl buffer, pH 7.4) were each treated with a solution of Pronase (0.88 mg/mL, 200 μL). Degradation of peptides was monitored using HPLC.